Evaluation of Early-Age Drying and Shrinkage Cracking in Slab Systems

by

Atharwa Samir Nimbalkar

A Thesis Presented in Partial Fulfillment
of the Requirements for the Degree
Master of Science

Approved April 2023 by the
Graduate Supervisory Committee:

Narayanan Neithalath, Co-Chair
Barzin Mobahser, Co-Chair
Subramaniam Rajan

ARIZONA STATE UNIVERSITY

May 2023

ABSTRACT

Concrete develops strength rapidly after mixing and is highly influenced by temperature and curing process. The material characteristics and the rate of property development, along with the exposure conditions influences volume change mechanisms in concrete, and the cracking propensity of the mixtures. Furthermore, the structure geometry (due to restraint as well as the surface area-to-volume ratio) also influences shrinkage and cracking. Thus, goal of this research is to better understand and predict shrinkage cracking in concrete slab systems under different curing conditions. In this research, different concrete mixtures are evaluated on their propensity to shrink based on free shrinkage and restrained shrinkage tests.

Furthermore, from the data obtained from restrained ring test, a casted slab is measured for shrinkage. Effects of different orientation of restraints are studied and compared to better understand the shrinking behavior of the concrete mixtures. The results show that the maximum shrinkage is near the edges of the slab and decreases towards the center. Shrinkage near the edges with no restraint is found out to be more than the shrinkage towards the edges with restraining effects.

ACKNOWLEDGMENTS

I would like to start by expressing my gratitude to my advisor Professor Narayanan Neithalath for giving me the opportunity to work with him. His guidance and support are the reasons I was able to accomplish this work. Thank you to Professor Barzin Mobasher and Professor Subramaniam D. Rajan for serving on my defense committee.

I would like to gratefully acknowledge financial support for this project received from SUNDT Construction. This project was conducted in the Structural Mechanics and Materials Testing laboratories at Arizona State University and as such I would like to acknowledge the support that has made these experiments possible. I would like to acknowledge the assistance of Mr. Jeff Long, the laboratories manager, and Mr. Peter Goguen, for assistance in performance and preparation of experimental testing.

In addition, I want to acknowledge the assistance of my colleagues at Arizona State University including, Avinaya Tripathi, Aswathy Simon, Sahil Surehali, and Rijul Kanth Ramasamy Jeyaprakash.

Thank you to all my friends who helped keep me sane during the process including Sharayu Thosar, Atharva Desale, Dishika Agrawal, Atharva Bendre, Khushboo Ramraje, Thilak Senthil, Ashutosh Maurya, and Mohammed Raihan.

I would finally like to express my deepest appreciation and gratitude to my family. I would like to thank my parents and my late grandfather for their love and support through my path of self-discovery. And finally, I would like to thank my parents for being a constant reminder to worry about the important things in life.

TABLE OF CONTENTS

Page

LIST OF TABLES v

LIST OF FIGURES vi

LIST OF EQUATIONS ix

LIST OF ABBREVIATIONS x

CHAPTER

1 INTRODUCTION 1

1.1. Background 1

1.2. Aims and Objectives 2

1.3. Research Methodology 3

1.4. Thesis Structure 4

2 LITERATURE REVIEW 5

2.1. Introduction 5

2.2. Types of Shrinkage 6

2.2.1. Drying Shrinkage 6

2.2.2. Autogenous Shrinkage 7

2.2.3. Thermal Shrinkage 8

2.2.4. Carbonation Shrinkage 9

2.3. Methods to Measure Shrinkage 9

2.3.1. Free Shrinkge Test 9

2.3.2. Restrained Ring Test 10

3 EXPERIMENTAL PROGRAM 12

CHAPTER Page

3.1. Materials and Mix Proportioning 12

3.2. Mechanical Properties 13

3.2.1. Compressive and Tensile Strength 13

3.2.2. Modulus of Elasticity 16

3.3. Shrinkage Testing 18

3.3.1. Free Shrinkage 18

3.3.2. Restrained Ring Test 19

3.3.3. Slab Shrinkage 24

4 RESULTS AND DISCUSSION 29

4.1. Compressive and Tensile Strength 29

4.2. Modulus of Elasticity 30

4.3. Ring Test Experimental Results 32

4.4. Material Property Development 34

4.5. Determination of Degree of Restraint 40

4.6. Slab Experimental Results 44

5 CONCLUSION 50

REFERENCES 52

LIST OF TABLES

Table Page

Table 1: Mixture Proportioning Of Designed Mixtures. 12

Table 2: Mechanical Properties Of NC And CPC Mix Obtained Experimentally. 31

Table 3:Regression Coefficients. 39

LIST OF FIGURES

Figure Page

Figure 1: 2.2.2.1 Reactions Causing Autogenous And Chemical Shrinkage. (Tazawa, 1999), C = Unhydrated Cement, W = Water, Hy = Hydration Products, And V = Voids Generated By Hydration. 8

Figure 2:3.2.1.1 Cylindrical Specimens Casted To Obtain The Mechanical Properties Of The Concrete Mix. 14

Figure 3: 3.2.1.2 Compression Testing Machine With Cylindrical Specimen Failed In Compression. 14

Figure 4: 3.2.1.3 A) Testing Machine And Setup For Split Tensile Strength B) Cylindrical Specimen Failed In Tension..... 15

Figure 5: 3.2.2.1 Testing Machine And Setup According To ASTM C469 To Calculate Modulus Of Elasticity. 16

Figure 6: 3.2.2.1 Various Steps Involved In Preparing The Ring For Restrained Ring Test. 1) Steel Ring Of Accurate Dimensions. 2) Smoothen The Inner Surface Of The Ring Using Sandpaper. 3) Apply Bonding Agent To Attach Strain Gage. 4) Attach The Strain Gage At Mid-Height With The Help Of Tape. 5) Provide Additional Tape To Ensure No Damage. 21

Figure 7: 3.2.2.2 Restrained Ring Test Setup With Four Strain Gages. 21

Figure 8: 3.2.2.3 Geometry Of The Steel Ring Used For Restrained Ring Test. 22

Figure 9: 3.2.2.4 A) Data Acquisition Chassis B) Strain Gage Module C) Assembly D) System..... 24

Figure Page

Figure 10: 3.3.3.1 A) Concrete Embedment Vibrating Wire Strain Gage (Geokon 4200). B) 8 Channel Vibrating Wire Mesh Node (Geokon Geonet 8900 Data Logger). C) System Used For Recording And Storing The Shrinkage Data. 25

Figure 11: 3.3.3.2 Top View Of The Wooden Mold Made In House To Cast A Slab With Special Arrangements. 27

Figure 12: 3.3.3.3 Side View Of The Wooden Mold Made In House To Cast A Slab With Special Arrangements. 28

Figure 13: 3.3.3.4 Pictures Taken During The Casting Of The Slab With SUNDT Workers And Calportland Truck. 28

Figure 14: 4.1.1 Compressive Strength Of NC And CPC Mixtures. 29

Figure 15: 4.1.2 Tensile Strength Of NC And CPC Mixtures. 30

Figure 16: 4.2.1 Comparison Of Theoretical And Experimental Modulus Of Elasticity. 31

Figure 17: 4.3.1 Strain Data From All Four Sensors Along With The Crack For The NC Mixture. 32

Figure 18: 4.3.2 Strain Data From All Four Sensors Along With The Crack For The CPC Mixture. 32

Figure 19: 4.3.3 Net Strain Against The Square Root Of Elapsed Time For Each Strain Gage. 34

Figure 20: 4.4.1 A) Regression Fits For NC Shrinkage Components B) Regression Fits For CPC Shrinkage Components. 35

Figure 21: 4.4.3a) Regression Fit To Calculate Regression Coefficients For NC Mixture. 38

Figure Page

Figure 22: 4.4.3b) Regression Fit To Calculate Regression Coefficients For CPC Mixture. 39

Figure 23: 4.5.1 Degree Of Restraint For NC And CPC Mixtures. 42

Figure 24: 4.5.2 Illustration Of The Idealization For Computing The Residual Stress In The Concrete. 43

Figure 25: 4.5.3 Residual Stress Development In Concrete Ring Specimen. 43

Figure 26: 4.6.1 Shrinkage Strain Measured In The Slab At Various Locations. 45

Figure 27: 4.6.2 A) Comparison Of Gage S1 And S4 B) Comparison Of Gage S2 And S3 C) Comparison Of Gage S5 And S8 D)Comparison Of Gage S6 And S7 45

Figure 28: 4.6.3 Comparison Of Measured Shrinkage Strains In Gages S1, S2, S5 And S6 46

Figure 29: 4.6.4 A) Comparison Of Shrinkage Strains Measured In Gages S1 And S2 B) Comparison Of Shrinkage Strains Measured In Gages S5 And S6. 47

Figure 30: 4.6.5 Comparison Of Shrinkage Strains Measured In Restrained And Unrestrained Portions Of The Slab. 48

Figure 31: 4.6.6 Tensile Stresses Developed In The Slab Compared To The Tensile Strength Obtained From Splitting Tension Test. 48

LIST OF EQUATIONS

Equation Page

Equation 1: Equation For Calculating Theoretical Modulus Of Elasticity. 17

Equation 2: Equation For Calculating Modulus Of Elasticity To The Nearest 50000 Psi According To ASTM C469. 17

Equation 3: Equation To Calculate Strain Rate Factor. 33

Equation 4:4.3.2 Equation To Calculate The Stress Rate. 34

Equation 5: Equation For Calculating Shrinkage Strains. 35

Equation 6: Equations Used To Fit The Data For Regression Coefficients. 36

Equation 7: 4.4.1 Modulus Ratio Vs Time And Tensile Strength Ratio Vs Time A) NC Mixture B) CPC Mixture. 37

Equation 8: Equation To Calculate Theoretical Elastic Stress. 40

Equation 9: Equations To Calculate The Constant C1R And C2R. 40

Equation 10: Equation To Calculate Shrinkage Of Inner Radius Of Concrete. 41

Equation 11: Equations Which Describes The Displacement At Outer Surface Of Steel Ring And The Inner Surface Of The Concrete Ring. 41

Equation 12:Equation To Determine The Degree Of Restraint. 41

Equation 13: Equation To Compute The Actual Residual Stresses. 43

Equation 14: Equation For Determining The Cracking Potential Of The Concrete Mix. 44

LIST OF ABBREVIATIONS

NC = Normal Concrete.

CPC = Calportland Concrete.

E = Modulus Of Elasticity.

F'c = Compressive Strength.

S_2 = Stress Corresponding To 40% Of Ultimate Load.

S_1 = Stress Corresponding To A Longitudinal Strain, ϵ_1, Of 50 Millionths (Psi).

ϵ_2 = Longitudinal Strain Produced By Stress S_2.

E = Strain [(In./In.), (M/M)].

A = Strain Rate Factor For Each Strain Gage, [(In./In.)/$Day^{1/2}$], [(M/M)/$Day^{1/2}$].

T = Elapsed Time, (Days).

K = Regression Constant.

Q = Stress Rate, [(Psi/Day), (Mpa/Day)].

G = $10.47x10^6$ Psi (72.2 Gpa).

$|A_{avg}|$ = Absolute Value Of The Average Strain Rate Factor [(In./In.)/$Day^{1/2}$].

$\Delta\epsilon_{sh}$ = Incremental Free Shrinkage.

E_c = Modulus Of Elasticity Of Concrete.

E_s = Modulus Of Elasticity Of Steel Ring.

ν_c = Poisson's Ratio Of Concrete (0.18).

ν_s = Poisson's Ratio Of Steel (0.30).

R_{IC} = Inner Radius Of Concrete Ring.

R_{OC} = Outer Radius Of Concrete Ring.

R_{IS} = Inner Radius Of Steel Ring.

R_{OS} = Outer Radius Of Steel Ring.

$\boldsymbol{\Delta}U_{SH}$ = Drying Or Autogenous Shrinkage Strain Of The Concrete Ring If The Restraining Effect Is Removed (Allowing Concrete To Shrink Freely).

$\Delta\epsilon_{sh}$ = Incremental Free Shrinkage.

Ψ = Degree Of Restraint.

$P_{residual}$ = Actual Residual Stress.

Θ_{CR} = Cracking Potential.

CHAPTER 1

INTRODUCTION

1.1.Background:

Concrete structures are built with the aim to utilize them for many years without losing their structural capacity. But due to shrinkage and associated cracking issues, concrete structures can deteriorate much faster during its service life. Shrinkage and cracking of concrete affect its strength and serviceability. For that reason, a comprehensive work is required to minimize shrinkage issues that could be introduced in the structure. The high risk of shrinkage cracking has been previously demonstrated based on high-performance concrete, because of the high cementing materials content (needed for high strength requirements), which influences the long-term durability of the structure.

Shrinkage cracking can occur throughout the concrete curing process, and even beyond; however early age shrinkage is critical and needs to be minimized. Predicting the chance of early age cracking in cementitious materials is a complicated and difficult task since there are many variables involved. These variables influence the rate of property development of concrete, as well as its interaction with the external environment, and in-turn highly influences the tendency of concrete to shrink. Moisture loss, heat of hydration, and thermal effects are majorly responsible for determining shrinkage in concrete. When shrinkage occurs in concrete structures restrained by supports, tensile stress develops in concrete and cracking occurs.

Shrinkage in concrete can occur at different stages. Plastic shrinkage manifests itself soon after the concrete is placed in the forms, while the concrete is still in its plastic

state. Drying shrinkage, which this work is focused on, starts after the final setting, and continues well into the life of the structure. However, it is more prominent in early stages when the concrete has not developed enough strength. Thus, the measurements in this study will go on until 14 to 28 days after concrete casting. While autogenous shrinkage is also an important concern, we will not carry out its measurement since the water-to-cement rations used in common construction is large enough to mitigate such concerns.

1.2.Aims and Objectives:

The aim of this research is to predict the shrinkage and cracking in slab systems, designed typically for water-retaining structures. Structures need to be highly crack resistant, and thus concrete mixture, structural design and construction procedures must be coordinated appropriately. Several complex coupling phenomena between the thermal strains and rate of property development influences cracking. In this work, the attempt is to understand the propensity of concrete mixtures to shrinkage cracking, and how slab geometries and time of casting (how long after the slab is casted), along with restraints influences concrete cracking. In this work, the shrinkage and cracking in the slab system is studied using restrained ring test (ASTM C1581), free shrinkage test (ASTM C157) and mechanical properties of the concrete mixtures.

The objectives were:

i. To conduct field monitoring of freshly casted slab, combined with small sample test (located on site and the in the lab) to help characterize material properties, to quantify the extent and timing of early age movements and the associated climatic conditions.

ii. To understand the effect of restraint on the internal movement of the slab, which takes account of appropriate parameters of the concrete mix, slab dimensions, restraint condition and the exposure to climatic conditions.

1.3.Research Methodology:

An extensive literature review identified little work on early age behavior of slabs; a range of relevant information on thermal and moisture induced concrete movements. Although there was little information available on early age shrinkage of slabs, a relevant body of work on the restraining effects and long-term shrinkage of smaller specimens was identified.

To understand the early age drying and shrinkage cracking of the concrete mixtures, restrained ring test was performed. The degree of restraint for the mixture was determined using this test and mechanical properties of the concrete. The mechanical properties of the concrete mix were obtained from compression test (ASTM C39), split tension test (ASTM C496) and elastic modulus test (ASTM C469). Additionally, from the data obtained from these tests, residual stresses in the concrete were calculated.

Initially, the temperature and relative humidity (RH) were identified as the parameters most likely to affect the behavior of the slabs. Instrumentation was chosen to monitor these internal temperatures of concrete. The movement of the concrete was recorded by vibrating wire strain gages, which were chosen for their stability, precision and sensitivity. The vibrating wire strain gages were connected to data logger which saved the recorded data into a computer.

1.4.Thesis Structure:

Chapter 1 outlines the background, aims and objectives of the research. It is an introduction to the thesis.

Chapter 2 presents the summary of earlier work on early-age drying and shrinkage cracking. Here, different types of shrinkage and their testing methods are studied.

Chapter 3 describes the selection and development of instrumentation used to measure and monitor early-age behavior of concrete. This chapter contains a detailed study of the tests performed. Furthermore, it also explains the procedure for all the tests performed in this study.

Chapter 4 contains the results from compression, tension and elastic modulus test. Additionally, it gives the analysis of the restrained ring test which provides the degree of restraint and residual stresses in concrete. On the other hand, this chapter provides insight on the comparison of shrinkage with different types of restraining effects.

Chapter 5 brings together the summaries and conclusions from chapters 3 and 4.

CHAPTER 2

LITERATURE REVIEW

2.1.Introduction:

Shrinkage of concrete is of crucial concern as the structures are built with the aim to utilize them for many years, without losing its structural integrity. However, over time cracking associated with shrinkage deteriorates the structure much faster in its service life. Shrinkage and cracking affects the strength and the serviceability of the structure. The volume changes in the structure are usually attributed to drying of the concrete over longer duration. Although recent studies have also focused on the early-age behavior of shrinkage problems (Holt, n.d.). The high risk of shrinkage cracking has been previously demonstrated based on high performance concrete, because of high cementing materials content (needed for high strength requirements), which influences the long-term durability of the structure.

Shrinkage cracking can occur throughout the concrete curing process, and even beyond; however early age shrinkage is critical and needs to be minimized (Aly & Sanjayan, 2009). Predicting the chance of early age cracking in cementitious materials is a complicated and difficult task since there are many variables involved. These variables influence the rate of property development of concrete, as well as its interaction with the external environment, and in-turn highly influences the tendency of concrete to shrink. Moisture loss, heat of hydration, and thermal effects are majorly responsible for determining shrinkage in concrete. When shrinkage occurs in concrete structures restrained by supports, tensile stress develops in concrete and cracking occurs.

2.2.Types of shrinkage:

Volume change in concrete is unavoidable thus, resulting in moisture loss in the environment as well as their internal reactions. The volume change due to environmental phenomenon is called drying shrinkage while the volume change due to internal reactions is called autogenous shrinkage. Other types of shrinkage are thermal shrinkage and carbonation shrinkage. Thermal shrinkage is the change in the volume due to the temperature fluctuations. While carbonation shrinkage is the process when cement paste in the hardened concrete reacts with the moisture and carbon-di-oxide in the air, in accordance with Equation 2. (Mehta, P. Kumar and J.M. Monteiro, n.d.)

2.2.1. Drying shrinkage:

Volume change due to loss of moisture is referred as drying shrinkage. The water in the concrete will evaporate due to the environment the concrete is exposed to. This water loss in the concrete will result in contraction of concrete. Thus, this contraction in concrete is known as the drying shrinkage (Drying Shrinkage, Curling, and Joint Opening of Slabs-on-Ground). After the concrete is cast, the larger particles, aggregates settle at the bottom allowing the water to rise towards the surface. This water is known as the bleed water. Bleed water from the surface will evaporate but the concrete will be subjected to drying. Therefore, the water is pulled out from the interior of the concrete mass. Due to this phenomenon, surface cracks are developed on the concrete. At early ages, the most common situation from drying shrinkage is the development of surface cracks. There might be also other problems with internal stresses or cracking due to water suction into the sub-base material (Sidney and young). Amount of drying shrinkage is dependent on the evaporation of moisture and the rate of evaporation. If the bleed water is evaporated

at a faster rate, there are higher chances of drying shrinkage. Whereas, if the rate of bleeding is higher than the rate of evaporation, the water will act as blanket to the concrete, avoiding it from cracking.

2.2.2. Autogenous shrinkage:

Autogenous shrinkage is defined as the volume change in the concrete at macroscopic level without any moisture transferred to the exterior surrounding environment. This type of shrinkage is the result of chemical shrinkage associated with the hydration of cement particles (Tazawa, 1999). Figure 2.2.2.1 shows a graphic depiction of the concrete's volume change due to the hydration of cement (Tazawa, 1999). Autogenous shrinkage is associated with chemical shrinkage, but chemical shrinkage is an internal volume reduction whereas, autogenous shrinkage is an external volume change. Autogenous shrinkage cannot be stopped by any casting or curing methods, but it needs to be addressed at the time of concrete mix proportioning. Other terms used in for autogenous shrinkage includes autogenous deformation, bulk shrinkage, indigenous shrinkage, self-desiccation shrinkage, Le Chatelier shrinkage, chemical shrinkage and autogenous volume change (Justnes et al., 1996).

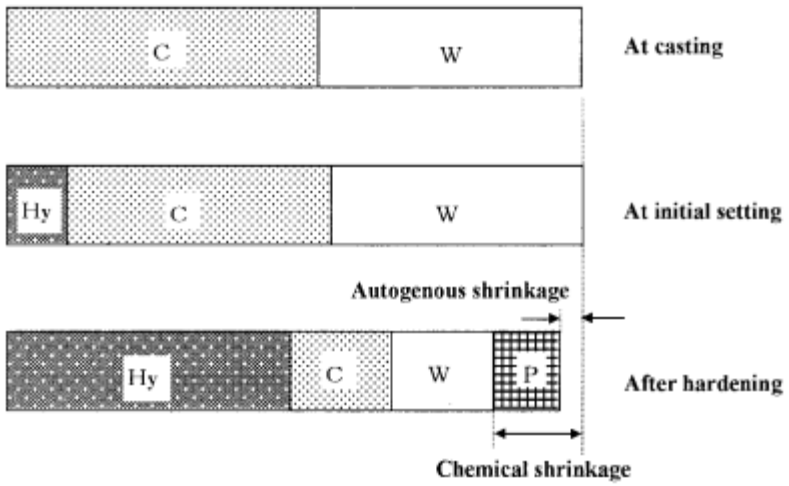

Figure 1: 2.2.2.1 Reactions causing autogenous and chemical shrinkage. (Tazawa, 1999), C = unhydrated cement, W = water, Hy = Hydration products, and V = voids generated by hydration.

2.2.3. Thermal shrinkage:

The volume change due to fluctuations in temperature is known as thermal shrinkage. The fluctuation in the temperature allows the concrete to expand with increase in temperature and contract with decrease in temperature. In places, where the temperature difference between daytime and nighttime is higher, the expansion and contraction in concrete is higher thus, resulting in problems. In early ages, due to the heat of hydration the interior temperature of the concrete is different than the surface temperature. This difference between the temperature within the concrete specimen and on the surface generates stresses and risk of cracking. Due to the heat of hydration, the temperature dilation in early ages is due to both surrounding temperature as well as the temperature in the concrete specimen. But, as temperature equilibrium is achieved between the surface

and the interior of the specimen, the temperature dilation is typically a result of temperature fluctuations in the surrounding environment.

2.2.4. Carbonation shrinkage:

Shrinkage is a long duration phenomenon and carbonation is the type which occurs in the longer run of the structures. When the cement paste in the hardened concrete reacts with the moisture and carbon-di-oxide available in the air (Mehta, P. Kumar and J.M. Monteiro) (Hlaing). Due to carbonation shrinkage, volume change occurs. But, in addition to this the pH of the concrete is reduced. The reduction in pH level of concrete can cause other problems such as corrosion of steel reinforcements. The corrosion of steel inside the concrete can cause cracking, expansion and spalling of the concrete (Design and Control of Concrete Mixtures).

2.3.Methods to measure shrinkage:

2.3.1. Free shrinkage test:

The free shrinkage test is performed according to the ASTM C157. This test method covers the determination of the length changes that are produced by causes other than externally applied forces and temperature changes in hardened hydraulic-cement mortar and concrete specimens made in the laboratory and exposed to controlled conditions of temperature and moisture. Measurement of length change permits assessment of the potential for volumetric contraction (shrinkage) of concrete due to drying. This test method is particularly useful for comparative evaluation of shrinkage potential in different hydraulic-cement mortar or concrete mixtures (Wongtanakitcharoen & Naaman, 2007). Assuming, the length of the specimens is much larger than the cross section, shrinkage

takes place only in the length direction. The length change measurement with time provides a measure of one-dimensional shrinkage of the material.

Some of the researchers have also measured the free shrinkage in concrete by using LVDTs. In this test method, the beam is casted in the steel rig and one end of the rig is fixed providing a fixed end for the concrete beam. The other side of the beam is not fixed but a LVDT is attached to the movable end and is connected to a computer to measure the movements of the beam due to shrinkage (Liu & Wei, 2021) (Liu et al., 2022). Some investigators have used the concrete embedment vibrating wire strain gages to measure the shrinkage in the concrete beams (Azenha et al., 2009) (Nam et al., 1947). In this study, a modified test setup of ASTM C157 is used to calculate the free shrinkage of the concrete beams. The procedure and the modifications are explained in further chapters.

2.3.2. Restrained ring test:

A steel ring for restrained shrinkage was done as early as 1939 to 1942 by Carlson and Reading (Carlson & Reading). The dimension of the concrete ring specimen they used was 25 mm thick and 38 mm wide casted around a 25 mm thick steel ring. The external diameter was 175 mm. Consequently, the concrete ring would shrink of drying, but the steel ring would provide restraint and prevent the ring from shrinking and thus, cracking occurs (Pease et al., 2023). Recently, instrumented rings are used by researchers to better quantify the early-age cracking tendency and to measure the tensile stresses that develop inside the material (Moon & Weiss, 2006) (Weiss et al., 2000) (Hossain & Weiss, 2006). Both, AASHTO and ASTM standards have developed the ring test due to its simplicity and economy. Major difference between these two standards is the relative ratio of concrete to

steel ring thickness which influences the degree of restraint provided to the concrete (Bakhshi). A ring-type restrained shrinkage testing method similar to ASTM standard is used in this chapter. This test method, although can be used to study cracking tendency of materials, it is not applicable to fresh concrete when plastic cracking is the main concern.

CHAPTER 3

EXPERIMENTAL PROGRAM

3.1.Materials and mix proportions:

The proportioning of designed mixtures is presented in Table 3.1.1**.** Here, for the normal concrete (NC) mix, aggregate to cement ratio of 2 was used to ensure early cracking of the ring. The maximum size of aggregate used in NC mix was 3/8 inches with cement content of 634.5 kg/m^3, medium sand content of 761.42 kg/m^3 and coarse aggregate content of 507.6 kg/m^3. The water to cement ratio of 0.5 was adopted for this mix.

The CPC mix was provided by CalPortland with cement content of 330 kg/m^3, size number 57 coarse aggregate content of 1055 kg/m^3, fine concrete sand content of 708 kg/m^3 and fly ash content of 83 Kg/m^3. The water to cement ratio of 0.42 was adopted. The specified slump of the mix was 5 to 8 inches.

Table 1: Mixture proportioning of designed mixtures.

Mix ID	NC	CPC
Portland cement (Kg/m^3)	635	330
Fine aggregates (Kg/m^3)	761	708
Coarse aggregates (Kg/m^3)	508	1055
Fly Ash (Kg/m^3)	-	83
Water (Kg/m^3)	317.5	42
w/c	0.5	0.42
Aggregate/cement	2	4.5

3.2.Mechanical properties:

Concrete is widely used material in construction industry due to its durability and strength. Mechanical properties are essential for proper use and design. Concrete exhibits different mechanical properties under different loading conditions. When loaded in compression, concrete has higher strength and withstands heavy load without failure. On the other hand, if loaded in tension, the strength of concrete is much lower compared to the compressive strength thus, resulting in failure in tension. The elastic modulus, described as the ability to elastically regain its original shape after the removal of load, is important to understand the deformation of concrete under different loads over time. Proper understanding of mechanical properties of concrete is required for the maintenance of the structure to ensure its durability and safety.

Several different test methods were performed to determine the age dependent properties which includes compressive strength, splitting tensile strength and elastic modulus of the concrete mixtures. Cylindrical specimens of size 100mm (4 in.) x 200mm (8 in.) were tested at different ages (1, 3, 5, 7, 14 days).

3.2.1. Compressive and tensile strength:

Standard concrete cylinders of size 100mm (4 in.) x 200mm (8 in.) were tested at different ages to measure the strength gain in concrete with time. Three specimens were tested at intervals of 1, 3, 5, 7 and 14 days to ensure repeatability. The average of the three specimens is reported in this research. The results indicates that the concrete strength increases as the concrete cures with time. The rate of curing is much faster early on and then slows down as shown in figure 4.1.1.

The compressive strength test of concrete was performed in accordance with ASTM C39. The specimen was loaded at the rate of 440 lbf/**s** until the cylinder fails in compression. The strength of both the concrete mixtures was increased with age. At the age of 14 days, the compressive strength of NC mixture obtained was 42 MPa whereas the strength for the CPC mixture was 38 MPa.

Figure 2:3.2.1.1 Cylindrical specimens casted to obtain the mechanical properties of the concrete mix.

Figure 3: 3.2.1.2 Compression testing machine with cylindrical specimen failed in compression.

The tensile strength was obtained for the same intervals as the compressive strength. ASTM C496 was followed to perform the tensile test. The loading rate applied was 120 lbf/s until the cylinder cracks. For NC and CPC mixtures, the tensile strength obtained at the age of 14 days was 3.62 MPa and 3.2 MPa respectively.

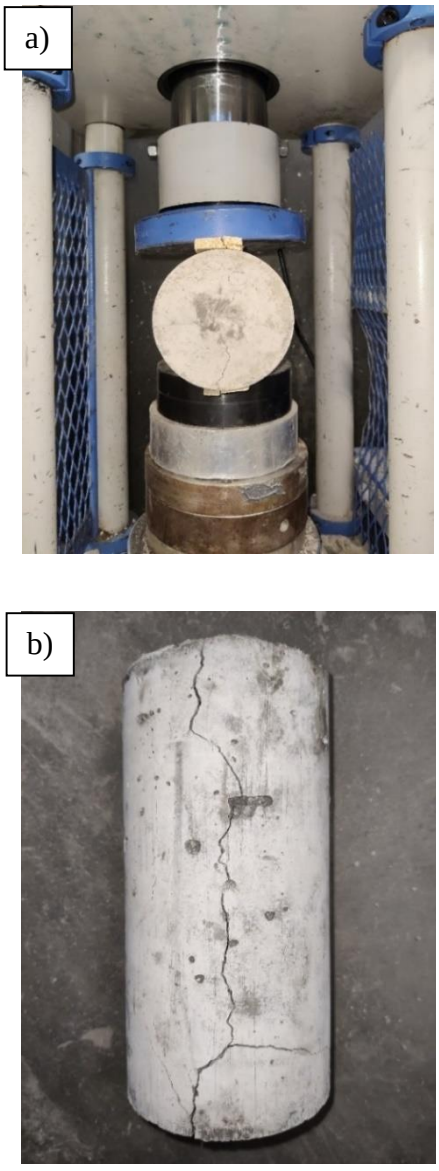

Figure 4: 3.2.1.3 a) Testing machine and setup for split tensile strength b) Cylindrical specimen failed in tension.

3.2.2. Modulus of elasticity:

Figure 5: 3.2.2.1 Testing machine and setup according to ASTM C469 to calculate modulus of elasticity.

The instrumented concrete cylinders were tested in compression at different ages (1, 3, 5, 7 and 14 days) to measure the modulus of elasticity. The test was performed according to ASTM C469. To achieve accurate results, the center of the specimen was aligned carefully with the center of the machine axis. The ends of the cylinders were covered with rubber pads to permit even stress distribution while applying load gradually to the specimen from 0% to 40% of the ultimate compressive load and removed gradually. The specimen was loaded and unloaded twice to ensure proper seating. After the first

loading cycle, primarily for the seating of the gages, corrections were made for any unusual behavior prior the second loading. A compressometer attached with dial gages was used to measure the deformation of the cylindrical specimen. The strain obtained from the dial gages was used to calculate the modulus of elasticity at different ages. Figure 4.2.1 shows the comparison between the modulus of elasticity obtained from the test and the modulus of elasticity obtained from equation 1. The modulus of elasticity, according to ASTM C469, to the nearest 50000 psi is calculated using equation 2.

$$E = 57000\ x\ \sqrt{f'c}$$

Equation 1: Equation for calculating theoretical modulus of elasticity.

where,

E = modulus of elasticity, and

f'c = compressive strength.

$$E = (S_2 - S_1)/(\epsilon_2 - 0.000050)$$

Equation 2: Equation for calculating modulus of elasticity to the nearest 50000 psi according to ASTM C469.

where,

E = chord modulus of elasticity, psi,

S_2 = stress corresponding to 40% of ultimate load,

S_1 = stress corresponding to a longitudinal strain, ϵ_1, of 50 millionths, psi, and

ϵ_2 = longitudinal strain produced by stress S_2.

3.3.Shrinkage testing:

3.3.1. Free shrinkage:

The free shrinkage test is performed according to the ASTM C157. This test method covers the determination of the length changes that are produced by causes other than externally applied forces and temperature changes in hardened hydraulic-cement mortar and concrete specimens made in the laboratory and exposed to controlled conditions of temperature and moisture. Measurement of length change permits assessment of the potential for volumetric contraction (shrinkage) of concrete due to drying. This test method is particularly useful for comparative evaluation of shrinkage potential in different hydraulic-cement mortar or concrete mixtures. In this test, a few modifications were made, beams of size 100mm (4 in.) x 100mm (4 in.) x 400mm (16 in.) and 150mm (6 in.) x 150mm (6 in.) x 525mm (21 in.) were used to enable a direct comparison to the results from the restrained ring test. Assuming, the length of the specimens is much larger than the cross section, shrinkage takes place only in the length direction. The length change measurement with time provides a measure of one-dimensional shrinkage of the material.

In this method, the specimens are cured under plastic sheet for the first 24 hours to protect the dripping water from the specimen. After 24 hours of casting, the specimens are demolded and placed in lime-saturated water maintained at 73 ± 1 °F for a minimum of 30 min before being measured for length. This is to minimize the variation in length due to variation in temperature. At an age of 24 ± ½ h after the addition of water to the cement during the mixing process, wipe the specimen with a damp cloth, and immediately take the initial comparator reading. After the initial reading, the specimens are stored in lime-saturated water at 73 ± 1 °F until they have reached an age of 7 days, including the period

in the molds. At the end of curing period, take the second comparator reading and store the specimens in a temperature-controlled room maintained at 104 ± 1 °F. To calculate the shrinkage strain, the difference between the average of readings on at least two specimens and the initial length of specimens is used. Since there is no restraining effect on the specimens, this test method cannot be an indicator of cracking performance of cement against shrinkage.

3.3.2. Restrained ring test:

If the prismatic specimen is restrained on the length direction, uniaxial tensile stresses are developed which is similar to a uniaxial tensile test. The data interpretation is relatively straightforward in linear specimen; however, it is difficult to provide sufficient restraint to produce cracking in linear specimens, especially when cross-sectional dimensions are large. It is also difficult to provide sufficient restraint to produce cracking with linear specimens, just as it is with uniaxial tensile test for concrete. Researchers have used long specimens with flared ends that are well restrained and used small cross-sectional dimensions to produce shrinkage cracking. Unfortunately for quality control procedures, these test methods are generally not useful due to difficulty in providing sufficient restraint. Various other specimen type has been used to simulate cracking due to restraint. (Kraai, P. P., 1985), (Shaeles & Hover, 1988), (Opsahl, O. A., & Kvam, S. F., 1982), and (Padron & Zollo, 1990) used a plate-type specimen. When restraint is provided in two directions, a biaxial state of stress is produced. As a result, the outcome obtained from plate-type specimen may depend on the specimen geometry and the material properties.

A steel ring for restrained shrinkage was done as early as 1939 to 1942 by Carlson and Reading (Carlson & Reading). The dimension of the concrete ring specimen they used

was 25 mm thick and 38 mm wide casted around a 25 mm thick steel ring. The external diameter was 175 mm. Consequently, the concrete ring would shrink of drying, but the steel ring would provide restraint and prevent the ring from shrinking and thus, cracking occurs. Recently, instrumented rings are used by researchers to better quantify the early-age cracking tendency and to measure the tensile stresses that develop inside the material. Both, AASHTO and ASTM standards have developed the ring test due to its simplicity and economy. Major difference between these two standards is the relative ratio of concrete to steel ring thickness which influences the degree of restraint provided to the concrete. A ring-type restrained shrinkage testing method similar to ASTM standard is used in this chapter. This test method, although can be used to study cracking tendency of materials, it is not applicable to fresh concrete when plastic cracking is the main concern.

This test method deals with the cracking resistance of the concrete mix subjected to drying shrinkage. Concrete shrinks due to loss of moisture from capillary and gel pore microstructure in hot and low humidity environments. Tensile stresses are developed when the concrete is restrained from free shrinkage. This result in cracking if the tensile stress exceeds the materials tensile strength. This is more dominant when at early age the tensile strength is low, and rate of moisture loss is high.

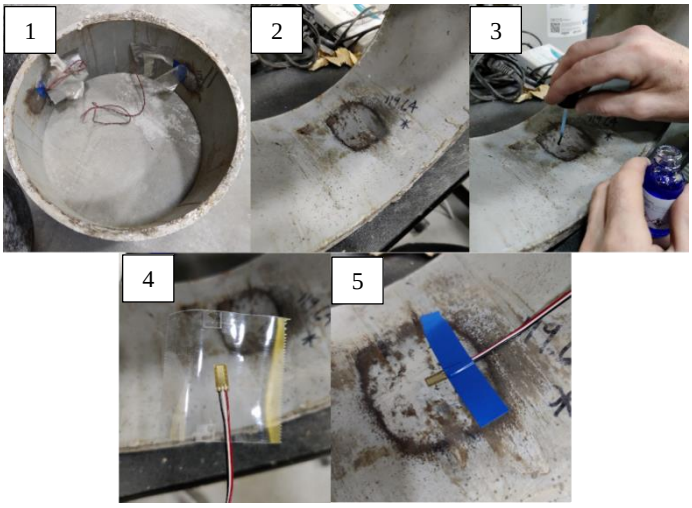

Figure 6: 3.2.2.1 Various steps involved in preparing the ring for restrained ring test. 1) Steel Ring of accurate dimensions. 2) Smoothen the inner surface of the ring using sandpaper. 3) Apply bonding agent to attach strain gage. 4) Attach the strain gage at mid-height with the help of tape. 5) Provide additional tape to ensure no damage.

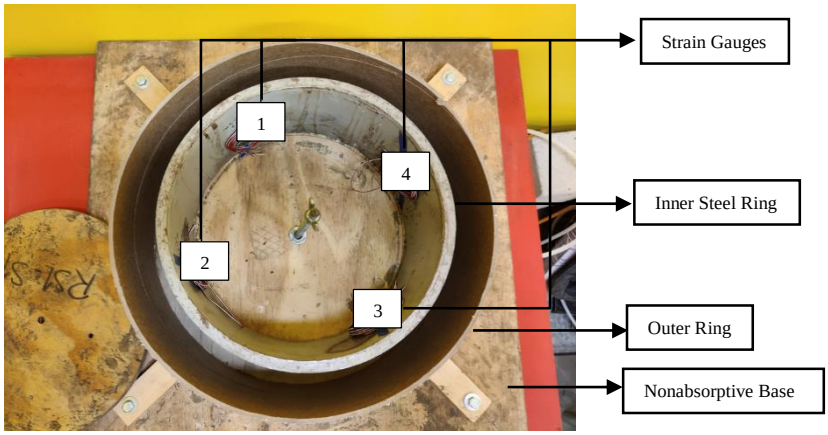

Figure 7: 3.2.2.2 Restrained ring test setup with four strain gages.

In this research, an instrumented ring similar to ASTM C1581 has been used to quantify the restrained shrinkage of the concrete mix. Figure 3.2.2.3 shows the schematic configuration and geometry of the ring specimen. A concrete ring with a thickness of 1.5 in. and a height of 6 in. is cast around a steel ring with a thickness of 0.5 in. The outer

diameter of the concrete ring is 16 in. To cast this simple specimen, a cardboard form is used to hold the concrete. The height of the specimen is much larger than the thickness of the concrete ring, it is assumed that uniform shrinkage takes place along the height of the specimen. A total of 4 strain gages as shown in Figure 3.2.2.2 are mounted on the interior surface of the steel ring at the mid-height level and 90 degrees apart to measure developed strains in steel due to shrinkage of concrete.

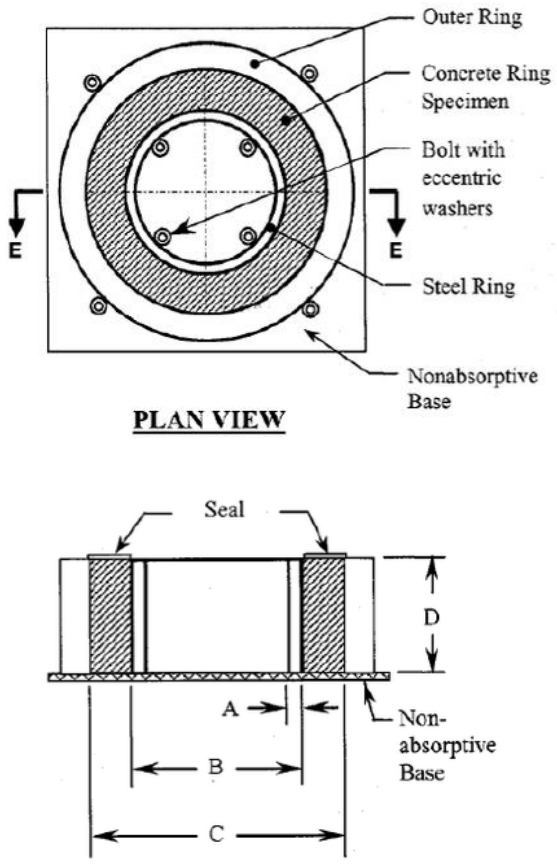

A	0.50 ± 0.12 in.
B	13.0 ± 0.12 in.
C	16.0 ± 0.12 in
D	6.0 ± 0.25 in.

Figure 8: 3.2.2.3 Geometry of the steel ring used for restrained ring test.

Two different concrete mixtures were used in this study to understand the drying and shrinkage cracking of the concrete mixtures. The mixing procedure adopted in this study is as follows. The dry materials including cement, and coarse and fine aggregates are introduced in the mixer and dry mixed for 2 mins. Then, water is added to the mixer thoroughly and blended for 5 mins. All the molds are filled in three layers with proper compaction by a tamping in between the layers. After the rings are filled completely, the ring was vibrated using a vibrating table, and the top surface was finished smooth.

Three replicate specimens are made from each batch of concrete. After casting, the specimens were moist-cured using a wet burlap at 73 ± 1 °F for 24 hours. After 24 hours of the addition of water into the cement, the specimens were demolded, the top surface of the ring samples was sealed by paraffin wax, and the outer cardboard form was removed. The removal of the cardboard form allowed drying to occur only from the outer circumferential surface of the concrete specimen. After sealing the top surface and removing of cardboard form, the samples were placed in the shrinkage chamber. The shrinkage chamber was maintained at constant humidity and at the temperature of 104 °F (40 °C). The strain gages attached to the inner surface of the steel ring was connected to the system to record the shrinkage. The response from the strain gages was collected using NI data acquisition devices and transferred into a LABVIEW-programmed computer. The program records the strain gages readings at specified intervals.

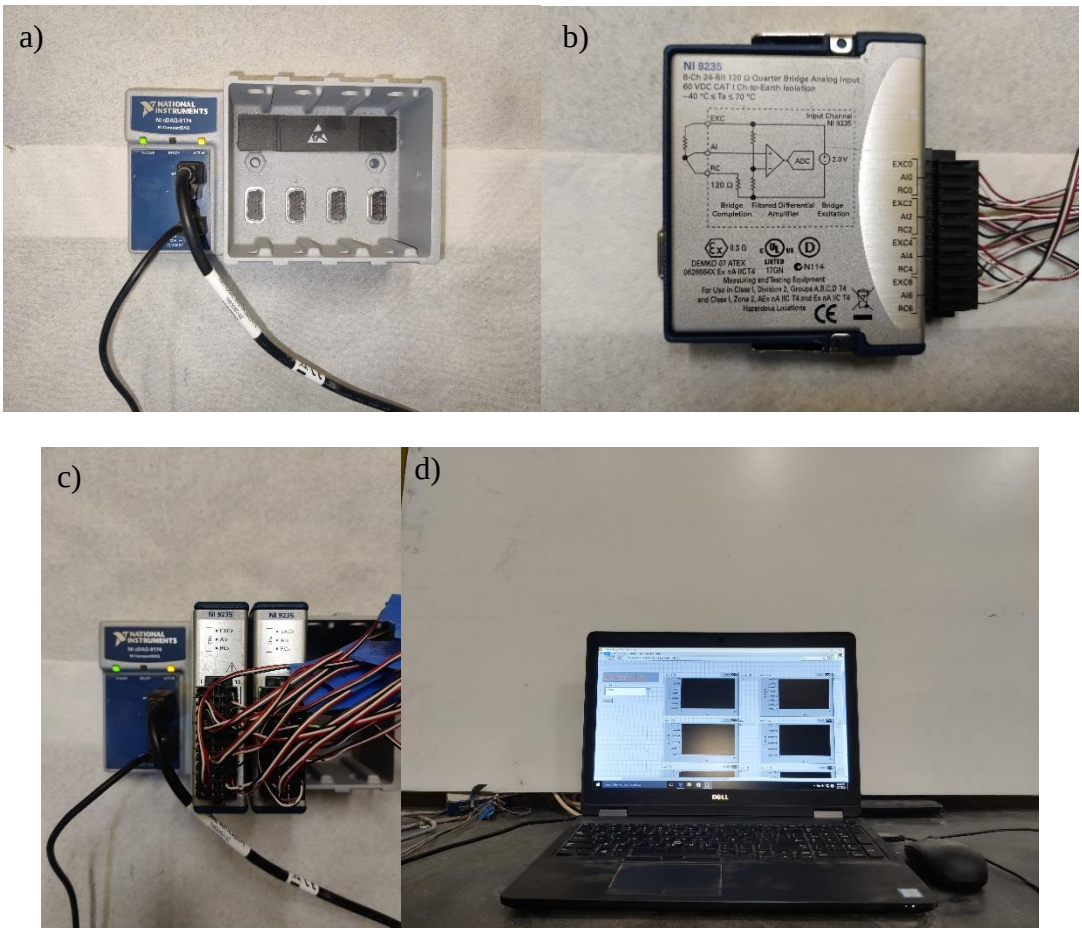

Figure 9: 3.2.2.4 a) Data acquisition Chassis b) Strain gage module c) Assembly d) System

3.3.3. Slab shrinkage:

In this study, the shrinkage of a slab at different locations in the slab was measured to understand the behavior of the concrete. Shrinkage is a crucial issue when it comes to concrete. Shrinkage occurs when the moisture in the concrete starts to evaporate, allowing the concrete to contract. Various factors affect the shrinkage in concrete slabs. Ambient temperature, internal temperature, and restraining effects are some of the examples which affect the movement of the slab at in early-ages. If the contraction of the concrete slab is

not taken into consideration, it can lead to cracking and other structural issues (curling of the slab) (Drying Shrinkage, Curling, and Joint Opening of Slabs-on-Ground).

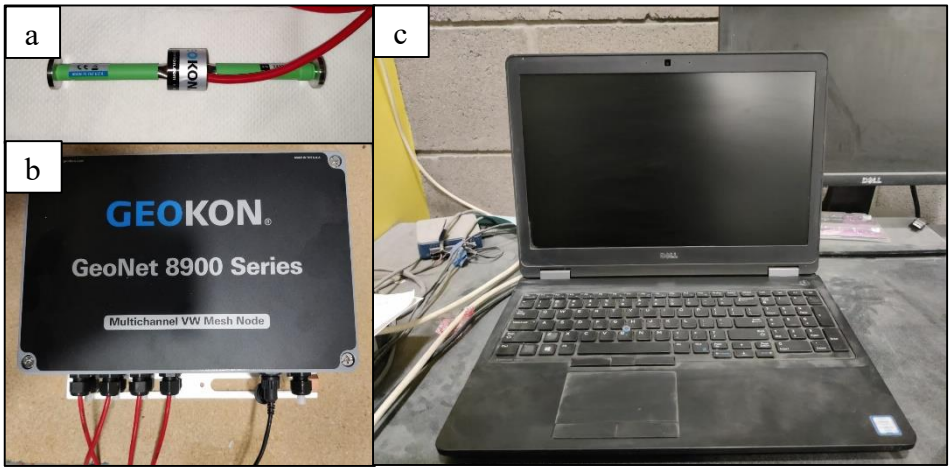

Figure 10: 3.3.3.1 a) Concrete embedment vibrating wire strain gage (Geokon 4200). b) 8 channel vibrating wire mesh node (Geokon GeoNet 8900 data logger). c) System used for recording and storing the shrinkage data.

Ambient temperature was identified as one of the major causes of shrinkage cracking in slabs (Bakhshi). In the daytime when the temperature is higher, the moisture loss in a slab is higher thus, resulting in more contraction of the slab. But, as the temperature cools down with the setting sun, the concrete tries to expand. This cycle of contraction and expansion causes stresses to develop in the concrete which results in the cracking of the slab. Places, where the difference between the daytime temperature and nighttime temperature is high, are most prone to cracking, if necessary, precautions are not taken.

The temperature of the concrete rises as soon as water is added to the cement. The reaction of cement with water is exothermic and causes heat to release. This increases the overall internal temperature of the concrete. In large concrete structural members like slabs,

the internal temperature can reach up to 158 °F (70 °C). The rise in the internal temperature of concrete results in moisture loss. This phenomenon is observed within the age of 1 day of the concrete. This causes rapid early shrinkage of the concrete mix.

The slab is usually restrained, thus not allowing the concrete to freely shrink and expand. This causes the slab to shrink more towards the center than towards the edges, where the slab is restrained. As the concrete tries to shrink but is restrained, tensile stresses are developed in the slab near the edges. Therefore, causing the slabs to propagate a crack through the edges. Conversely, if the slab is not restrained, it causes the slab to curl. The curling of the slab is the deformation of the slab in a curved shape with upward or downward bending of the edges. To summarize, the measurement of shrinkage in concrete slabs is crucial for ensuring their structural integrity, durability, and overall quality of the slab.

To quantify the shrinkage in the concrete slab, a large slab was cast, and vibrating wire strain gages were placed at different locations. Vibrating wire strain gages were adopted due to their precision, durability, and sensitivity. A wooden mold was instrumented to cast a slab with dimensions 8 ft. x 4 ft. x 0.5 ft. Figure 3.3.3.2 gives a detailed drawing of the mold. The mold was made in such a fashion that the half mold, i.e., a C-section (Figure 3.3.3.2) of the mold could be removed after 1 day of casting. This arrangement of the mold provided a comparison between unrestrained and restrained (due to the mold) shrinkage in the concrete slab. A total of eight vibrating wire strain gages were installed in the slab at mid-height (0.25 ft.) and connected to 8 channel data logger (Figure 3.3.3.1 b)

which recorded and downloaded the data on a computer. Figure 3.3.3.2 shows the orientation of the vibrating wire strain gages in the slab.

The mix design used for the slab was provided by CalPortland (CPC). The slab was poured from the truck and finished by the SUNDT Construction workers for us. Figure 3.3.3.4 shows the pictures taken on the day of the slab pour. The slab was poured at noon, and within 1 hour of pouring, strain gages were installed in the slab at mid-height. The data acquisition was started as soon as the strain gages were installed in place. The data was continuously recorded to understand the movement of the slab with time.

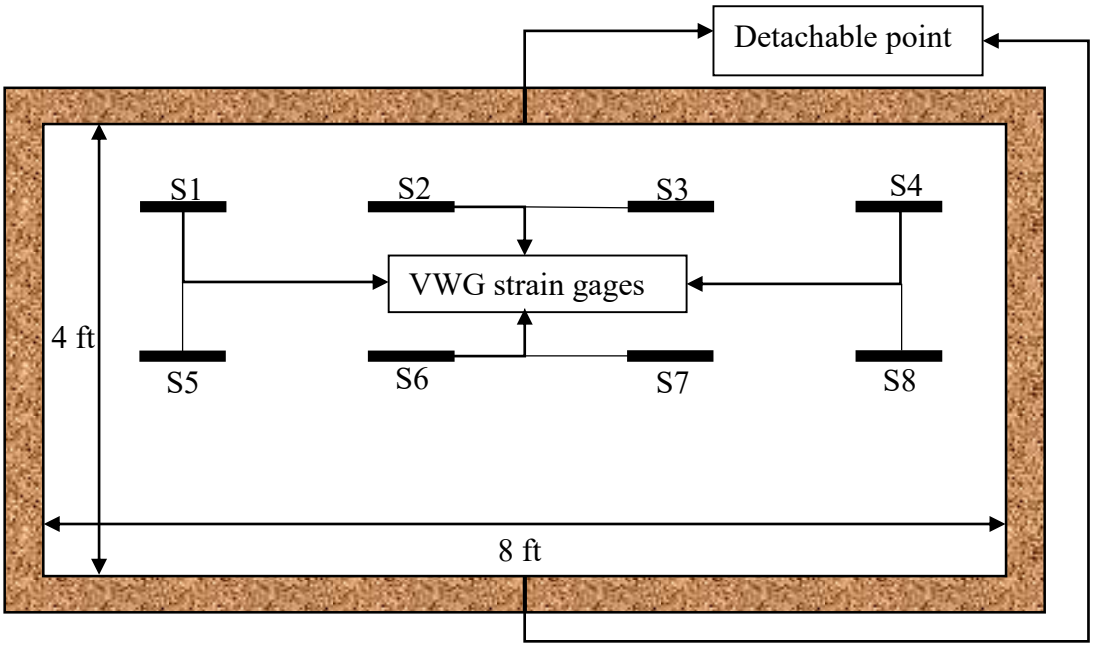

Figure 11: 3.3.3.2 Top view of the wooden mold made in house to cast a slab with special arrangements.

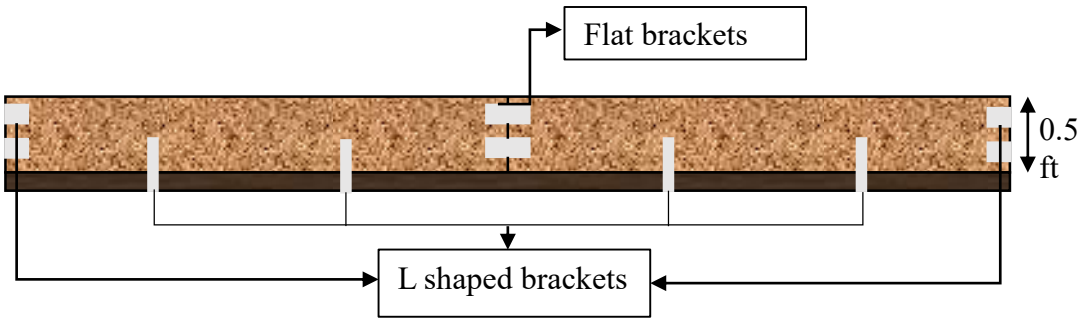

Figure 12: 3.3.3.3 Side view of the wooden mold made in house to cast a slab with special arrangements.

Figure 13: 3.3.3.4 Pictures taken during the casting of the slab with SUNDT workers and CalPortland truck.

CHAPTER 4

RESULTS AND DISCUSSION

4.1.Compressive and tensile strength:

Compressive strength test results are shown in Figure 4.1.1. The compressive strength of the concrete increases as the concrete cures with time. The rate of curing is much faster early on and then slows down as shown in Figure 4.1.1. The compressive strength reported is the average of the three specimens tested at each interval (1, 3, 5, 7, and 14 days) for every concrete mix. At the age of 14 days, the NC mix developed a strength of 42 MPa as compared to that of the CPC mix which developed 38 MPa. At an early age (1, 3, and 5 days), the strength of the NC mixture obtained was 17 MPa, 24 MPa, and 28 MPa respectively. On the other hand, the early-age (1, 3, and 5 days) compressive strength for the CPC mixture was obtained as 16 MPa, 25 MPa, and 31 MPa.

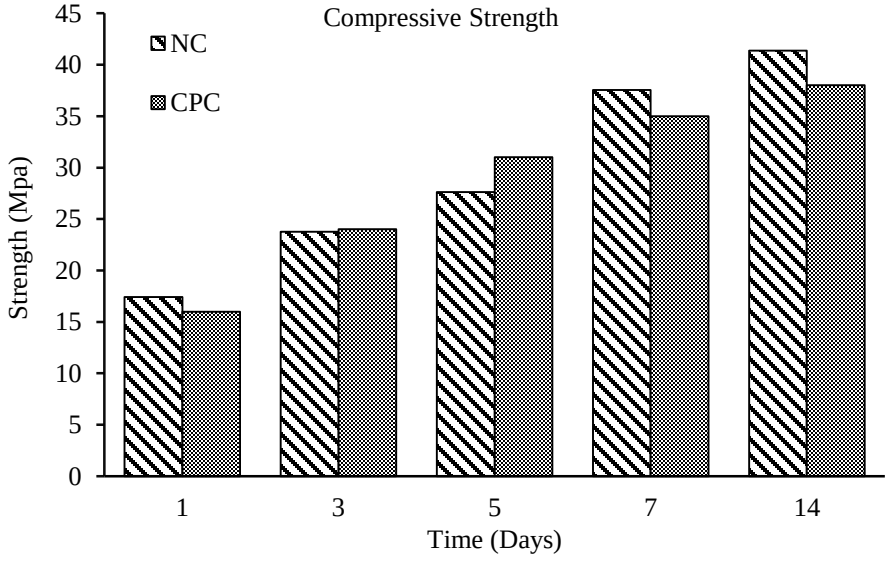

Figure 14: 4.1.1 Compressive strength of NC and CPC mixtures.

The tensile strength of concrete compared to compressive strength is much lower. Concrete is known to be strong in compression, but it fails (cracks) in tension early. The tensile strength is typically 10% of the compressive strength at the same age. The tensile strength obtained for the NC mixture at the age of 14 days was 3.62 MPa while for the CPC mixture was 3.2 MPa. Figure 4.1.2 shows the development of tensile strength in NC and CPC mixtures. The strength does not develop much, and the strength obtained for both the concrete mixtures is approximately 10% of its compressive strength at 14 days of age.

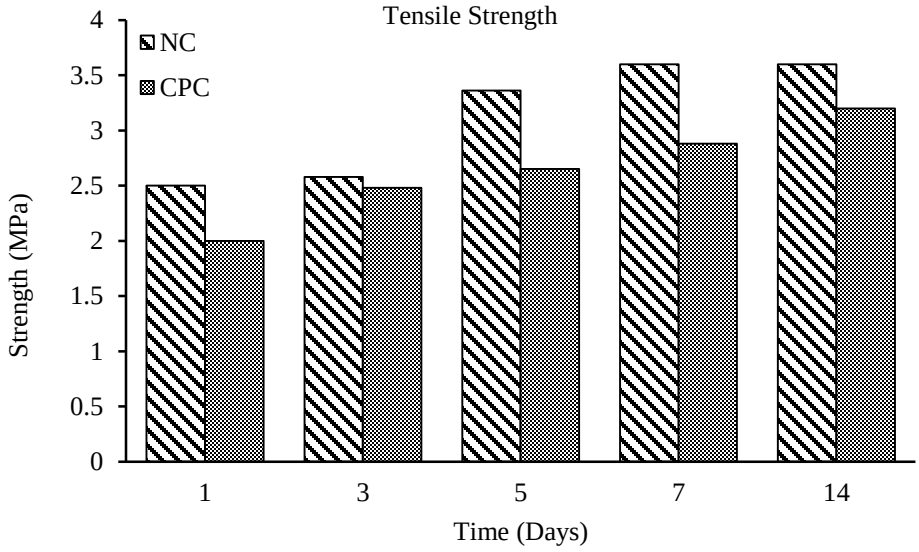

Figure 15: 4.1.2 Tensile strength of NC and CPC mixtures.

4.2.Modulus of elasticity:

Modulus of elasticity is the ability of a material to elastically regain its shape when the load is removed from the sample. Typically, the modulus elasticity of concrete is in the range of 30 to 50GPa. Compared to steel (190 to 210 GPa), the modulus of elasticity of concrete is much lower. In this study, the modulus of elasticity is calculated at different intervals of 1, 3, 5, 7, and 14 days. The values obtained from the test are compared to the theoretical values calculated using Equation 1**.** It is clearly visible in Figure 4.2.1, for both

NC and CPC mixtures, the E value obtained by the test method is higher than the value calculated using the equation. For the NC mixture, the modulus of elasticity at the age of 14 days was 34 GPa whereas for the CPC mixture was 40 GPa. The values of modulus of elasticity for both, NC and CPC mixtures, were obtained within the range of 30 to 50 GPa.

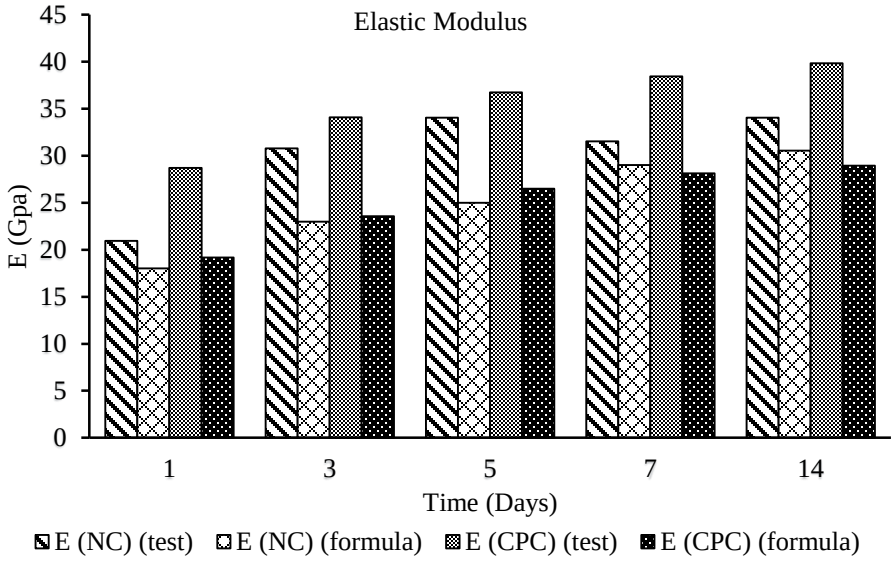

Figure 16: 4.2.1 Comparison of theoretical and experimental modulus of elasticity.

Table 2: Mechanical properties of NC and CPC mix obtained experimentally.

	NC			CPC		
Age	Compressive Strength	Tensile Strength	Modulus of Elasticity	Compressive Strength	Tensile Strength	Modulus of Elasticity
(Days)	(MPa)	(MPa)	(GPa)	(MPa)	(MPa)	(GPa)
1	17	2.51	21	16	2	29
3	4	2.58	30	25	2.5	34
5	28	3.36	34	31	2.65	37
7	37	3.6	32	36	2.88	39
14	41	3.62	34	38	3.20	40

4.3.Ring test experimental results:

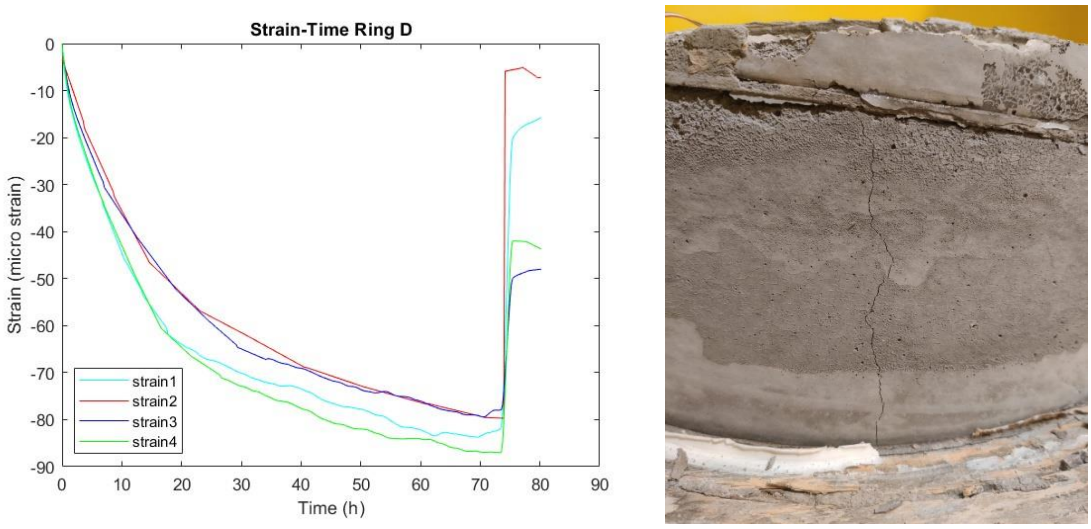

Figure 17: 4.3.1 Strain data from all four sensors along with the crack for the NC mixture.

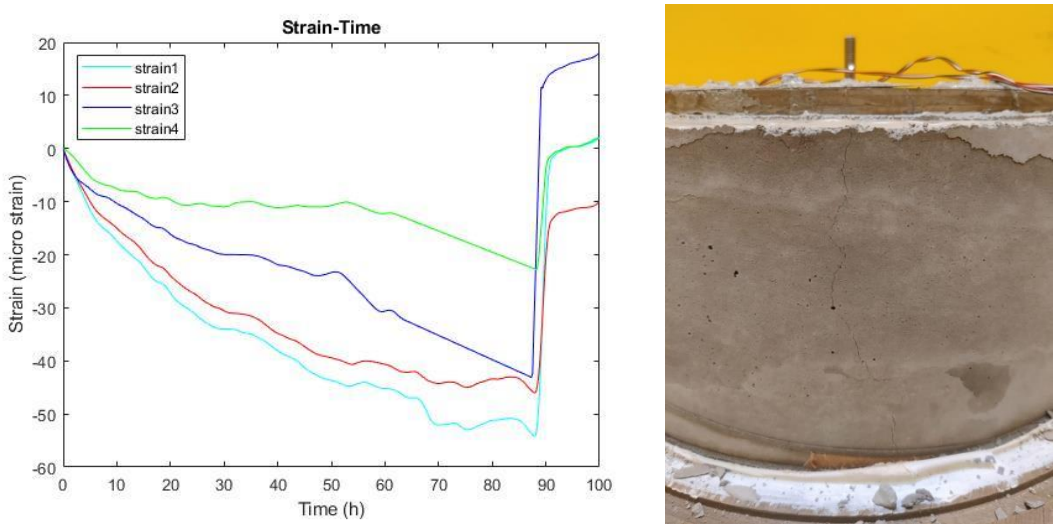

Figure 18: 4.3.2 Strain data from all four sensors along with the crack for the CPC mixture.

Figure 4.3.1 provides a graphical representation of the strain data obtained from 4 strain gages for the NC mixture attached to the ring using the data acquisition system along

with the picture of crack in the concrete ring. It can be noticed that the strain data abruptly reduces to zero in all four strain gages at an age of 74 h. This implies the age of cracking of the concrete. At the age of cracking, the average strain value is 82 micro-strains with the maximum strain in strain gage 4 (88 micro-strains). While figure 4.3.2 shows that the CPC concrete ring cracked at the age of 90 hours. The highest strain recorded in the ring was about 55 micro-strains. The strain rate factor (α); the slope of the fitted strain vs. square root of elapsed time for each strain gage can be calculated using equation 3.

$$\varepsilon = \alpha\sqrt{t} + k$$

Equation 3: Equation to calculate strain rate factor.

where,

ε = strain [(in./in.), (m/m)].

α = strain rate factor for each strain gage, [(in./in.)/day$^{1/2}$], [(m/m)/day$^{1/2}$].

t = elapsed time, (days).

k = regression constant.

The strain rate factor, obtained from the above strain data are -8.75, -9.22, -9.00, and -9.48 for strain gage 1 (S1), strain gage 2 (S2), strain gage 3 (S3), and strain gage 4 (S4) respectively. The average strain rate factor obtained was -9.11. The stress rate obtained from the data was 27.22 psi/day. The stress rate (q) was calculated using equation 4.

$$q = \frac{G\,|\alpha_{avg}|}{2\sqrt{t_r}}$$

Equation 4: Equation to calculate the stress rate.

where,

q = stress rate, [(psi/day), (MPa/day)].

G = 10.47×10^6 psi (72.2 GPa).

$|\alpha_{avg}|$ = absolute value of the average strain rate factor [(in./in.)/day$^{1/2}$].

t_r = elapsed time

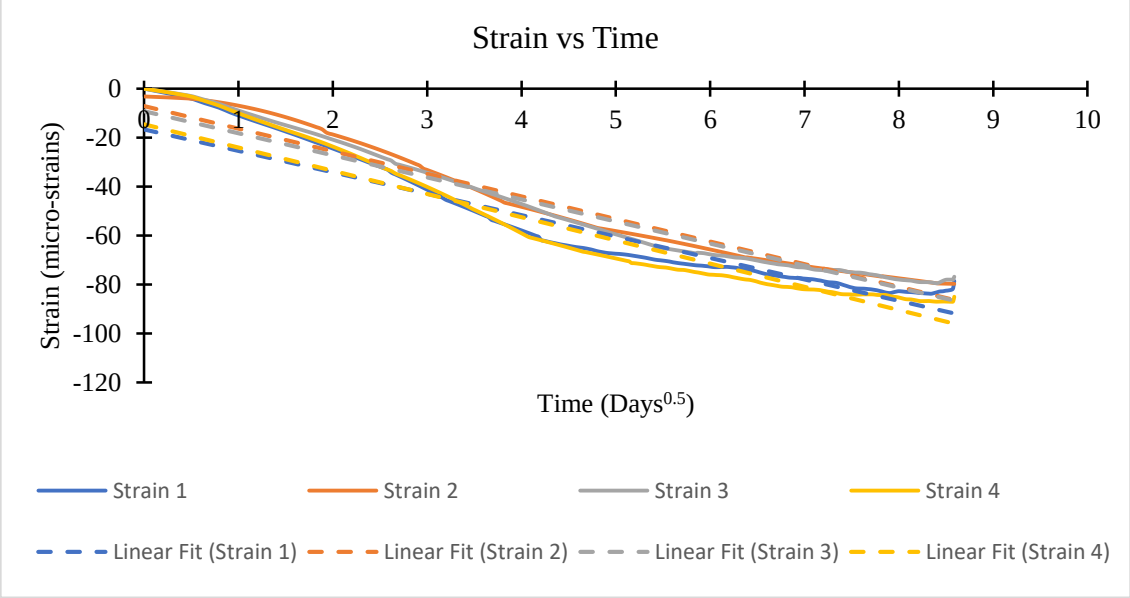

Figure 19: 4.3.3 Net strain against the square root of elapsed time for each strain gage.

4.4. Material property development:

Figure 4.4.1 shows the results of free shrinkage obtained from experiments that were performed to describe these materials. Since these experimental results correspond to measured properties at specific times, regression functions were developed to provide a

method that could represent the time-dependent material properties at other ages. The free shrinkage strain measurement is represented using equation 5 (Hossain & Weiss, 2004).

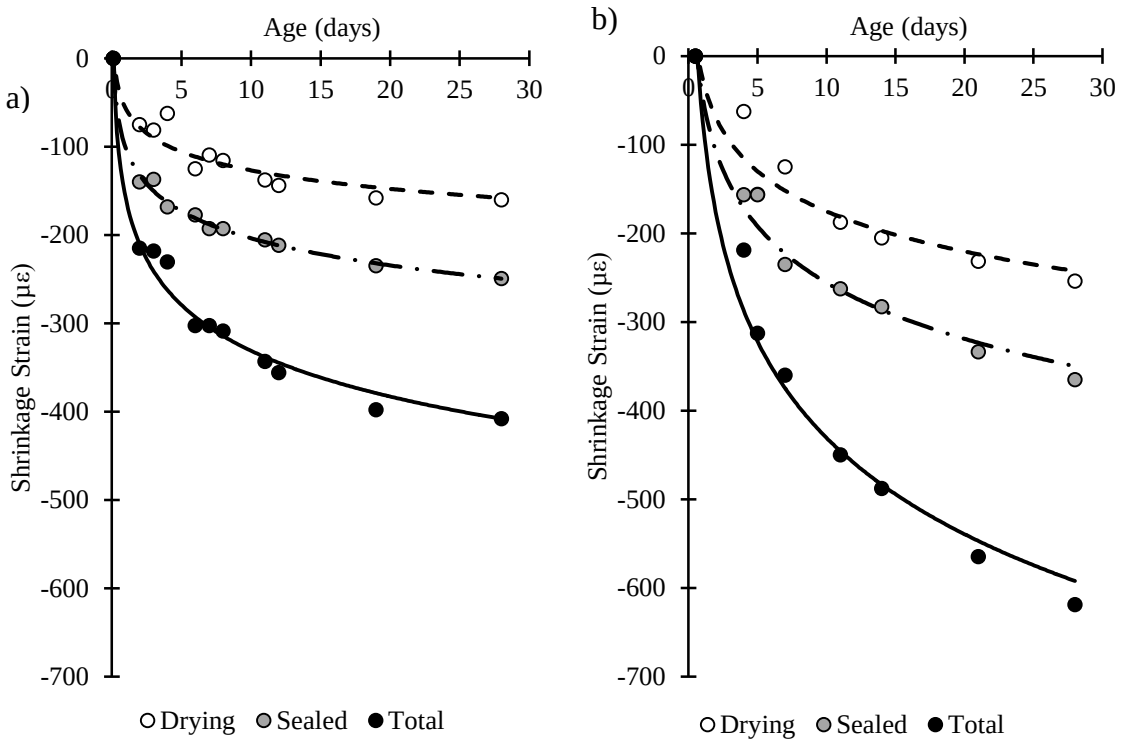

Figure 20: 4.4.1 a) Regression fits for NC shrinkage components b) Regression fits for CPC shrinkage components.

$$\varepsilon(t)_{SH} = C_1(t - t_o)^{C_2} + C_3\sqrt{t - t_d}$$

Equation 5: Equation for calculating shrinkage strains.

In this equation C1, C2, and C3 represent material constants, t is the age of the specimen, to represent the age of the specimen at setting (time zero), and td represents the age of the specimen when drying is initiated (1 day). The above equation is based on the approximation that total shrinkage is the sum of an autogenous component (first term) and a drying component (second term). The shape of the second term is based on the

observation of Acker (as reported by RILEM TC-69) (Bazant, 1986). The equation assumes that the drying and autogenous shrinkages are independent, which simplifies data analysis, though it should be noted that this is not absolutely true. To obtain the material constants, the following equations are fit:

$$\varepsilon(t)_{Sealed} = C_1(t - t_o)^{C_2}, \text{ and } \varepsilon(t)_{Drying} = C_3\sqrt{t - t_d}$$

Equation 6: Equations used to fit the data for regression coefficients.

Additionally, to determine the development of free shrinkage, expressions were fit to assess the elastic modulus and split tensile strength as shown in Figures 4.4.2a and 4.4.2b for mix NC and CPC respectively. To obtain a realistic value of rate constant, C4, the maximum static elastic modulus (E∞) for a mixture was determined from the intercept of a modulus versus the inverse of the time graph.

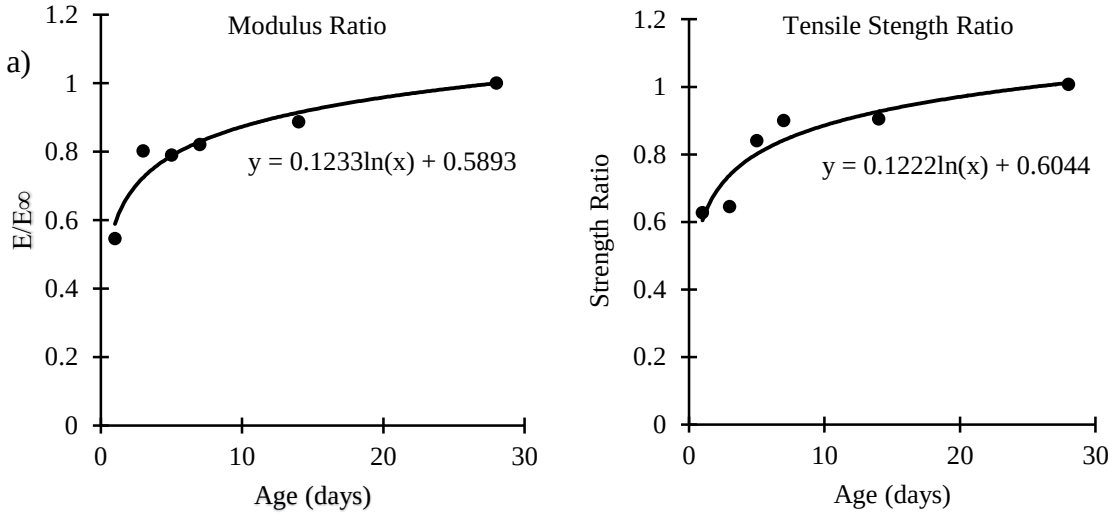

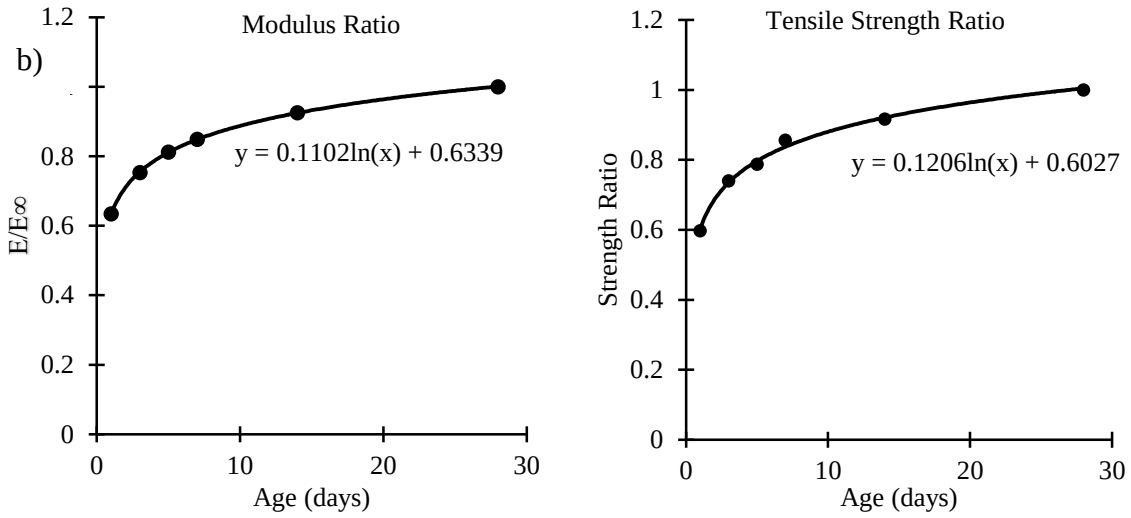

Equation 7: 4.4.1 Modulus ratio vs time and tensile strength ratio vs time a) NC Mixture b) CPC mixture.

$$E(t) = E_{\infty} \frac{C_4(t - t_o)}{1 + C_4(t - t_o)}$$

Similarly, the rate constant for split tensile stress can be shown to have a similar gain. As a result, the rate constant C_4 can be used to describe the rate of splitting tensile strength gain as well.

$$f_{sp}(t) = f_{sp\infty} \frac{C_4(t - t_o)}{1 + C_4(t - t_o)}$$

Figure 4.4.3a and 4.4.3b shows the regression fit for reciprocal strength and reciprocal elastic modulus to the reciprocal age along with the quantity $E/(E_{\infty} - E)$ and $f_{sp}/(f_{sp\infty} - f_{sp})$ against age. Table 3 shows the values of regression coefficients C_1 to C_4, E_{∞}, and $f_{sp\infty}$ for the NC and CPC concrete mixtures.

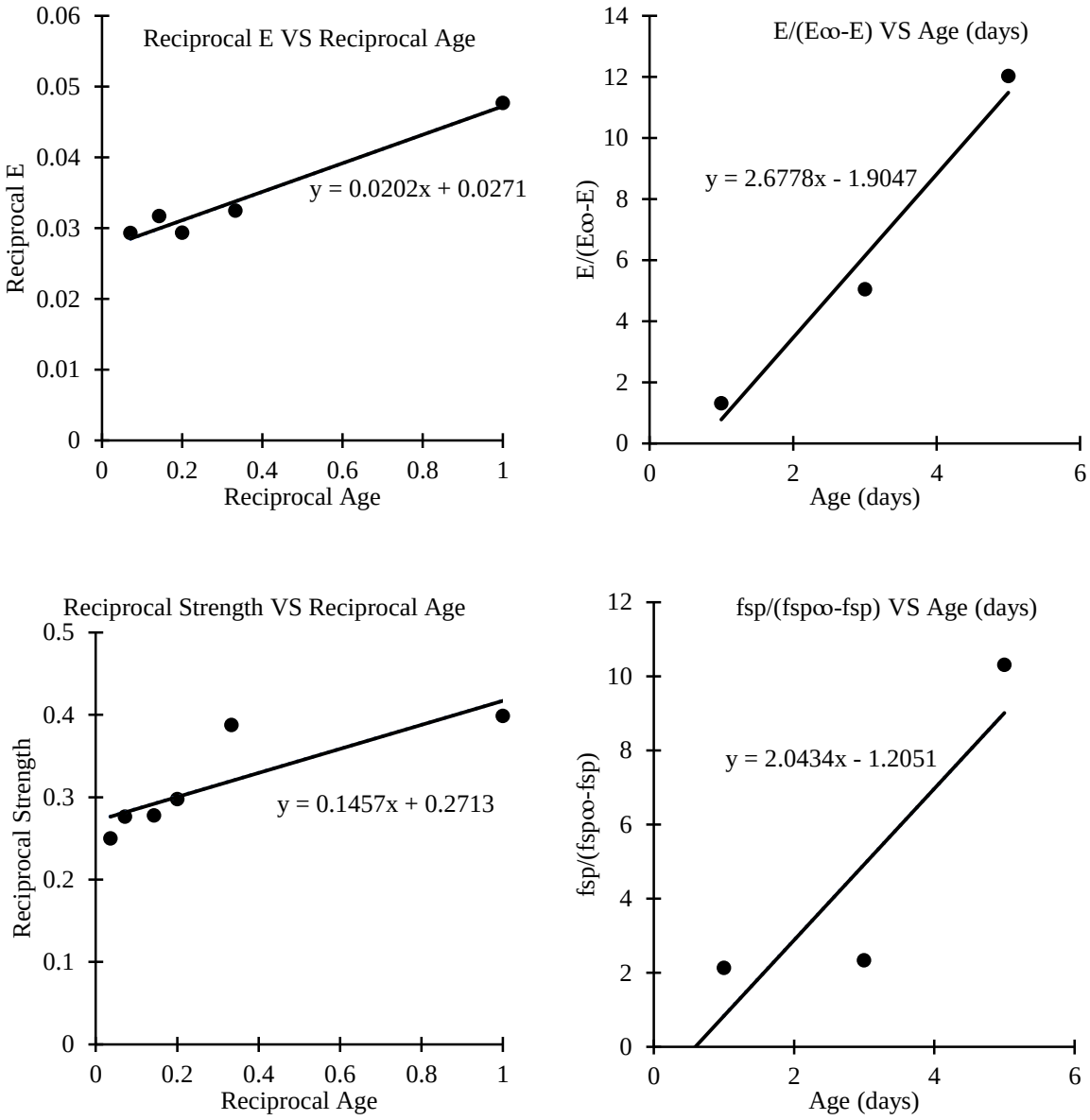

Figure 21: 4.4.3a) Regression fit to calculate regression coefficients for NC mixture.

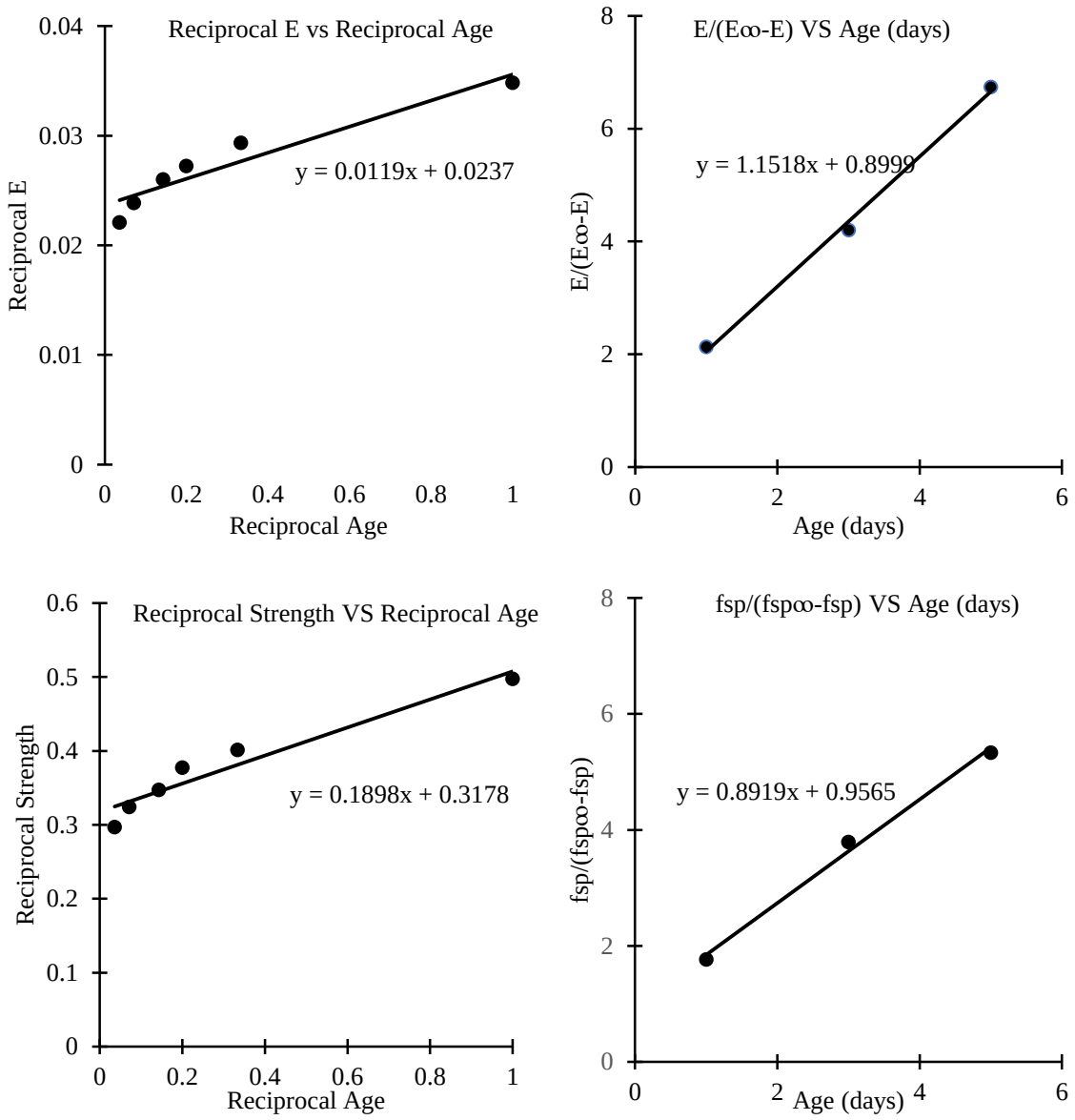

Figure 22: 4.4.3b) Regression fit to calculate regression coefficients for CPC mixture.

Table 3:Regression Coefficients.

Mixture	C_1	C_2	C_3	C_4	E_∞ (Gpa)	$F_{sp\infty}$ (Mpa)
NC	-75.55	0.42	-43.55	2.67	37	3.66
CPC	-37.92	0.83	-97.66	1.15	42	3.25

4.5.Determination of degree of restraint:

To determine the degree of restraint, theoretical elastic stress was calculated using equation 8 (Hossain & Weiss, 2004). In this equation, C1R and C2R can be assumed to be constant for a given geometry as shown in equation 9, and if Poisson's ratio for concrete is assumed to not vary as a function of time (vc = 0.18) (Hossain & Weiss, 2004).

$$\Delta p_{\text{elas}} = -\frac{\Delta \varepsilon_{\text{SH}} E_{\text{C}}}{\frac{E_{\text{C}}}{E_{\text{S}}} C_{1R} + C_{2R}}$$

Equation 8: Equation to calculate theoretical elastic stress.

$$C_{1R} = \frac{\left[(1+\nu_{\text{S}})R_{\text{IS}}^2 + (1-\nu_{\text{S}})R_{\text{OS}}^2\right]}{(R_{\text{OS}}^2 - R_{\text{IS}}^2)}$$

$$C_{2R} = \frac{\left[(1-\nu_{\text{C}})R_{\text{OS}}^2 + (1+\nu_{\text{C}})R_{\text{OC}}^2\right]}{(R_{\text{OC}}^2 - R_{\text{OS}}^2)}$$

Equation 9: Equations to calculate the constant C1R and C2R.

where,

$\Delta\epsilon_{SH}$ = incremental free shrinkage,

E_c = Modulus of elasticity of concrete,

E_s = Modulus of elasticity of steel ring,

v_c = Poisson's ratio of concrete (0.18),

v_s = Poisson's ratio of steel (0.30),

R_{IC} = inner radius of concrete ring,

R_{OC} = outer radius of concrete ring,

R_{IS} = inner radius of steel ring,

R_{OS} = outer radius of steel ring.

In addition to determining the elastic stress, using equations 10,11 and 12, the degree of restraint in the ring can be evaluated. Previous investigations (Shah et al., 1998) (Bentur et al., 2001) have discussed the importance of degree of restraint on cracking potential.

$$\Delta U_{SH} = R_{IC} \cdot \Delta\varepsilon_{SH}$$

Equation 10: Equation to calculate shrinkage of inner radius of concrete.

$$U_S|_{R_{OS}} = -\Delta p_{elas} \frac{R_{OS}^2\left[(1+\nu_S)R_{IS}^2 + (1-\nu_S)R_{OS}^2\right]}{E_S R_{OS}(R_{OS}^2 - R_{IS}^2)}$$

$$U_C|_{R_{IC}} = \frac{\Delta p_{elas}}{E_C} \cdot \frac{R_{IC}^2\left[(1+\nu_C)R_{OC}^2 + (1-\nu_C)R_{IC}^2\right]}{R_{IC}(R_{OC}^2 - R_{IC}^2)}$$

Equation 11: Equations which describes the displacement at outer surface of steel ring and the inner surface of the concrete ring.

$$\psi = \frac{U_{SH} - U_S|_{R_{OS}}}{U_{SH}} * 100\%$$

Equation 12:Equation to determine the degree of restraint.

where,

ΔU_{SH} = drying or autogenous shrinkage strain of the concrete ring if the restraining effect is removed (allowing concrete to shrink freely),

$\Delta\epsilon_{SH}$ = incremental free shrinkage,

R_{IC} = inner radius of concrete ring,

R_{OC} = outer radius of concrete ring,

R_{IS} = inner radius of steel ring,

R_{OS} = outer radius of steel ring,

Ψ = degree of restraint.

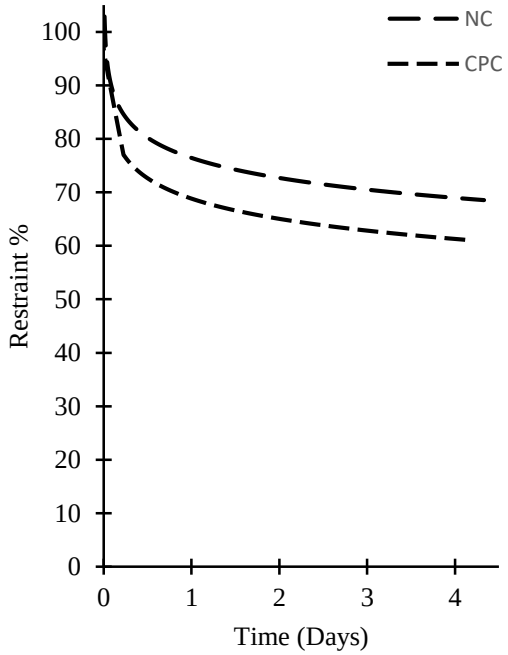

Figure 23: 4.5.1 Degree of restraint for NC and CPC mixtures.

Figure 4.5.1 illustrates the computed degree of restraint for the mixtures investigated in this study. First, it can be clearly seen that the degree of restraint varies with time due to the variation in the elastic modulus of the concrete (Hossain & Weiss, 2004). Second, the comparison of NC (w/c = 0.55) and CPC (w/c = 0.42) shows that the degree of restraint provided by the steel ring was more for the NC mixture than for the CPC mixture. It can be seen that the degree of restraint varies by approximately 8-10% due to the difference in elastic moduli described earlier in this study.

Figure 4.5.2 illustrates the idealization for computing the residual stress in the concrete. To determine the actual residual stress that develops in concrete, separate the ring

into a concrete cylinder pressurized at the inner surface and a steel cylinder pressurized with equal and opposite pressure at the outer surface.

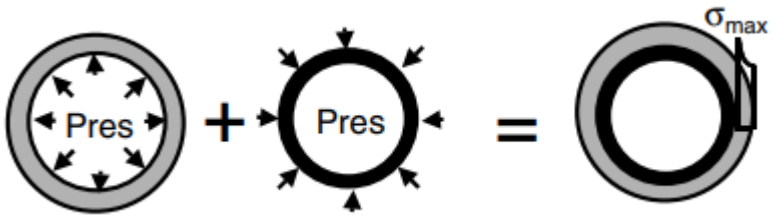

Figure 24: 4.5.2 Illustration of the idealization for computing the residual stress in the concrete.

The actual residual stress ($\rho_{Residual}$) can be computed as the pressure required to cause a strain that is equivalent to the measured strain in the steel ring (ε_{steel})(Hossain & Weiss, 2004) and is given by equation 13.

$$\rho_{\text{Residual}}(t) = -\varepsilon_{steel}(t).E_S.\frac{(R^2{}_{OC} - R^2{}_{IS})}{2R^2{}_{OC}}$$

Equation 13: Equation to compute the actual residual stresses.

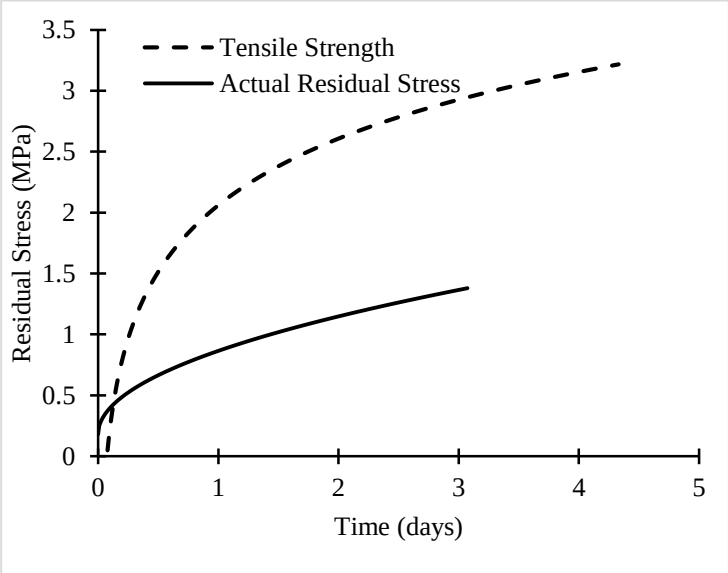

Figure 25: 4.5.3 Residual stress development in concrete ring specimen.

By comparing the obtained residual stress with the strength of a material provides a powerful tool to determine the cracking potential (Θ_{CR}) (i.e., the measure of how close the specimen may be to failure). The ability to measure the cracking potential may be important in cases where cracking is not observed experimentally. The cracking potential is based on the simple ratio of the actual residual stress and the splitting tensile stress (Equation 14). While it is common to think that failure may be expected to occur when the cracking potential reaches 1, experimental evidence typically shows that cracking takes place at lower values (RILEM).

$$\Theta_{\mathrm{CR}} = \frac{\sigma_{Actual-Max}}{f_{sp}(t)}$$

Equation 14: Equation for determining the cracking potential of the concrete mix.

4.6. Slab experimental results:

After casting the slab, the slab was covered with a plastic sheet to reduce moisture loss and to allow the hydration of cement. After one day, the plastic sheet was removed, and the slab was allowed to dry. Figure 4.6.1 shows the shrinkage strain in the concrete slab up till the age of 1.5 days. Maximum shrinkage strains were recorded in strain gages S5 and S8. This was obtained due to the restraining effect of the wooden mold on the edges of the concrete slab. Due to similar restraining effects, similar shrinkage strains were recorded in strain gages S1 and S4, S2 and S3, S5 and S8, and S6 and S7. Figure 4.6.2 shows the shrinkage strains measured in S1 and S4, S2 and S3, S5 and S8, and S6 and S7.

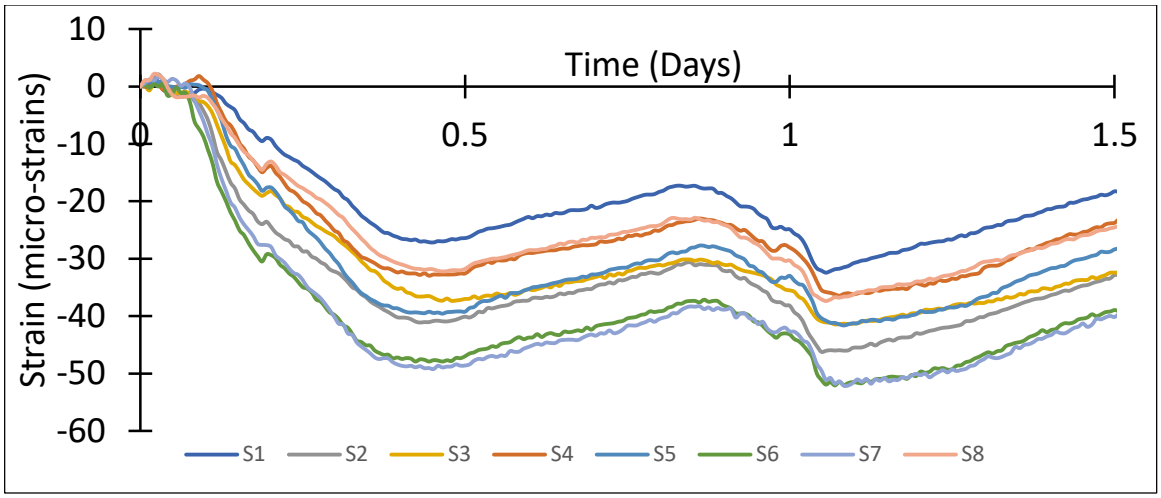

Figure 26: 4.6.1 Shrinkage strain measured in the slab at various locations.

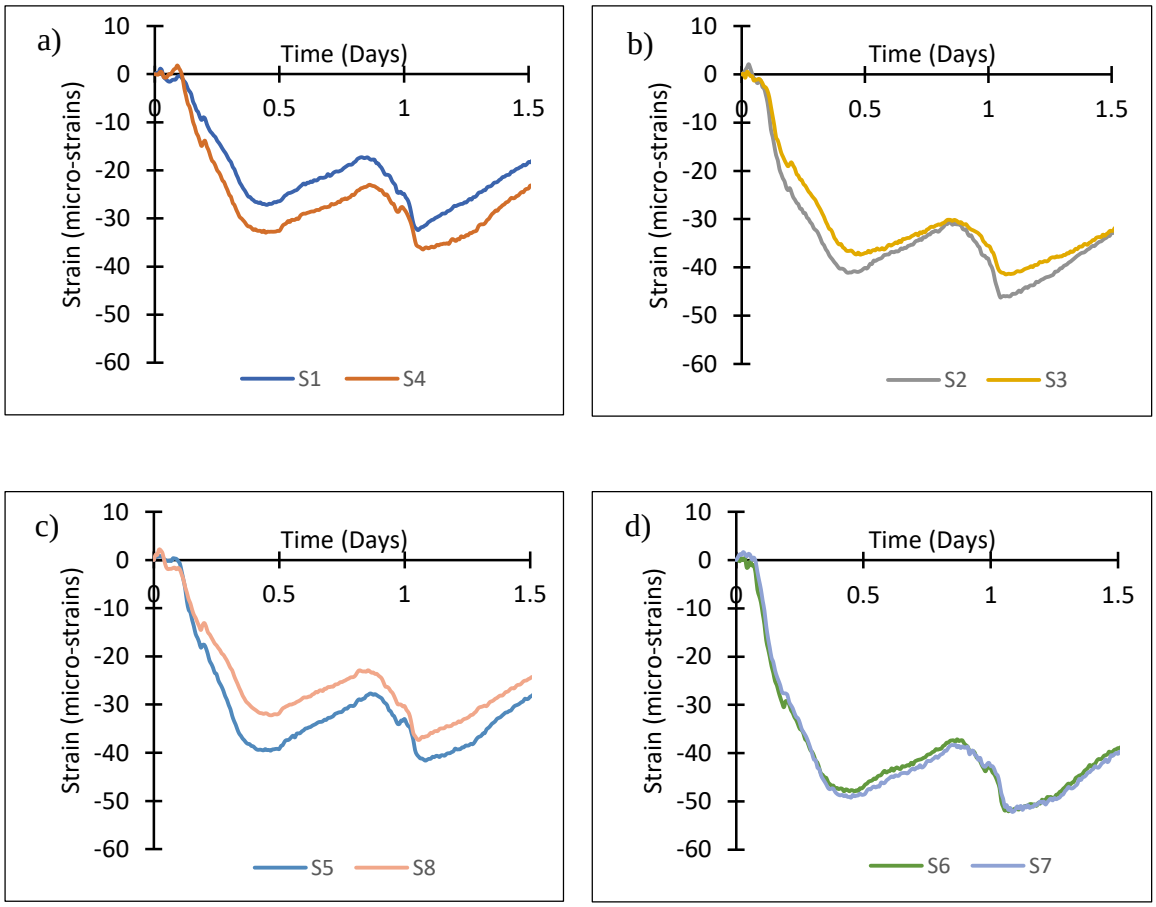

Figure 27: 4.6.2 a) Comparison of gage S1 and S4 b) Comparison of gage S2 and S3 c) Comparison of gage S5 and S8 d)Comparison of gage S6 and S7

For the early-age shrinkage in the slab, the shrinkage obtained in S1, S2, S5, and S6 were similar to S3, S4, S8, and S7 respectively. Thus, further, the shrinkage strains from one set of the above two were compared. Figure 4.6.3 shows that the strain gauge at the center of the slab (S6) recorded the highest shrinkage strain. Furthermore, the comparison of shrinkage along the edge of the slab is shown in Figure 4.6.4. Along the edge of the slab, the shrinkage strains appeared to be increasing (Liu & Wei, 2021). This was obtained due to more restraint on gage S1 than on gage S2. Similarly, the shrinkage strains measured in gage S5 were lesser than the shrinkage strains in gage S6.

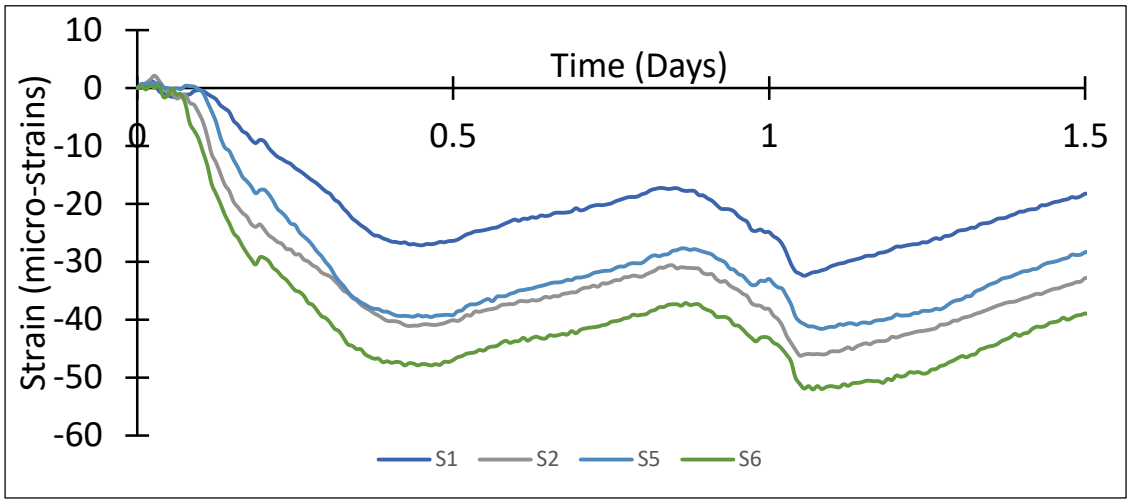

Figure 28: 4.6.3 Comparison of measured shrinkage strains in gages S1, S2, S5 and S6

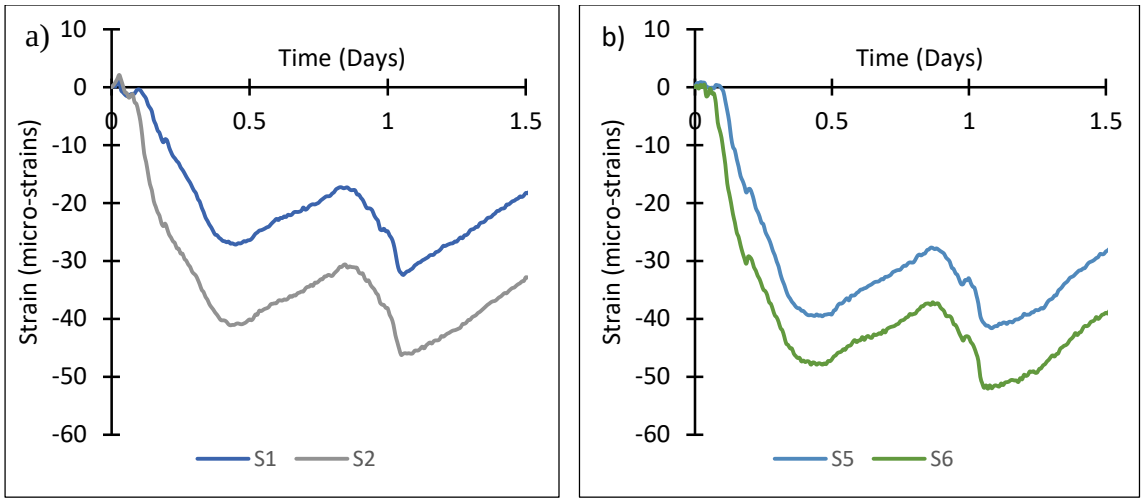

Figure 29: 4.6.4 a) Comparison of shrinkage strains measured in gages S1 and S2 b) Comparison of shrinkage strains measured in gages S5 and S6.

To quantify the shrinkage in the slab with different restraining effects, the wooden mold from one-half of the slab was removed. This arrangement provided no restraint to the slab near strain gages S3, S4, S7, and S8 whereas, the other half of the slab was restrained by the mold. Figure 4.6.5 shows the comparison between the gages after a portion of the slab was unrestrained. It is clearly seen that the movement of the slab in the restrained portion is less than in the unrestrained. The difference observed between the shrinkage of strain gages S2 and S3 was seen to be gradually increasing from 5 micro-strains to 25 micro-strains with time.

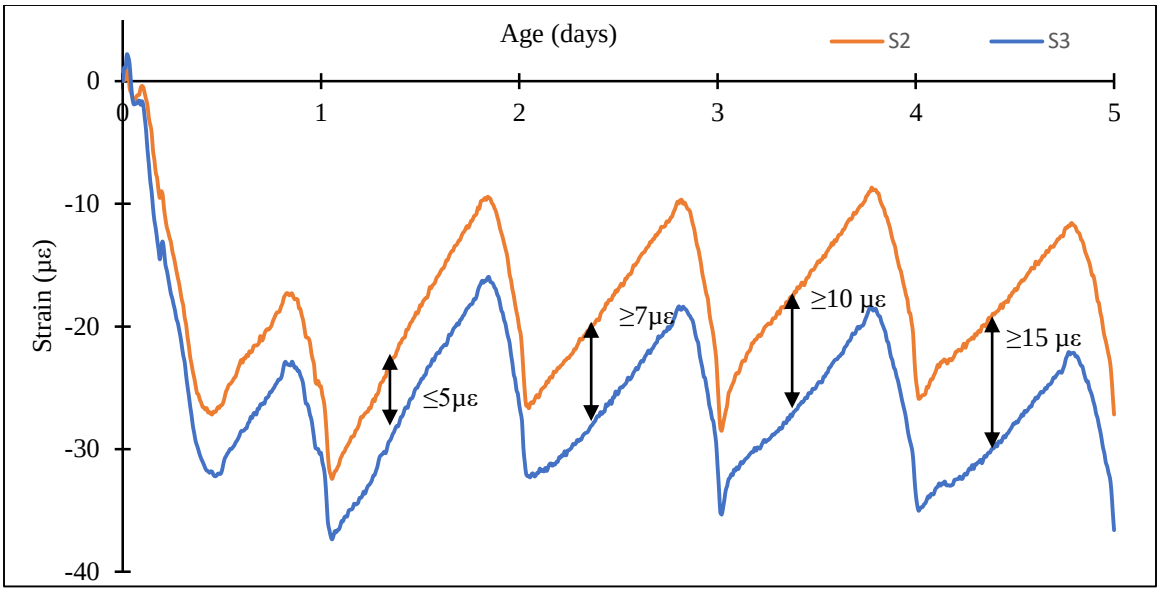

Figure 30: 4.6.5 Comparison of shrinkage strains measured in restrained and unrestrained portions of the slab.

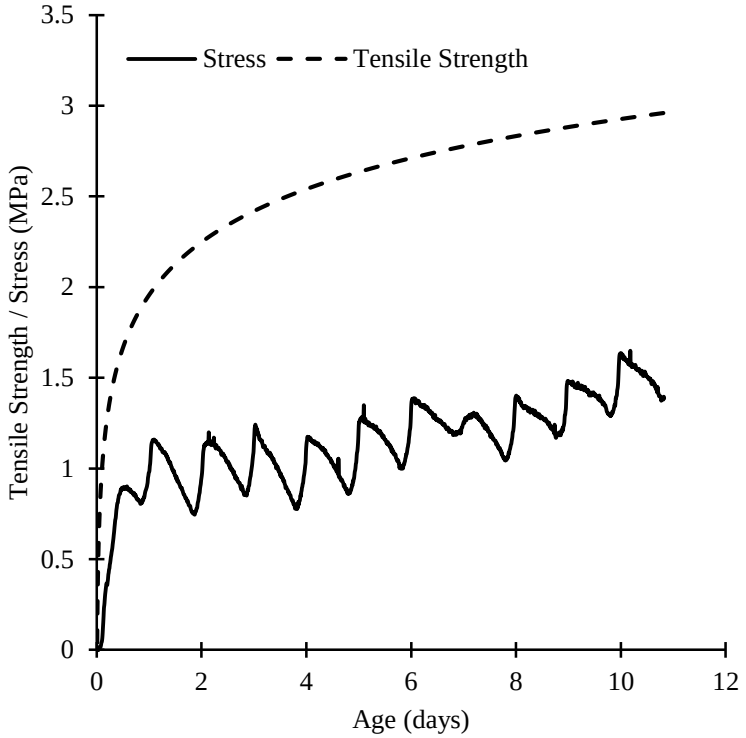

Figure 31: 4.6.6 Tensile stresses developed in the slab compared to the tensile strength obtained from splitting tension test.

While the previous discussion was based on the comparison between the shrinkage strains at different locations in the slab, figure 4.6.6 provides insights into the tensile stresses produced in the slab. The concrete cracks when the ratio of the tensile stress in concrete to the tensile strength reaches 1 (i.e., the stress produced in the concrete is equal to or greater than the tensile strength). At the age of 11 days, the maximum tensile stresses in the slab have been observed to be 1.65 MPa whereas, the tensile strength of the concrete mix obtained from split tensile strength was approximately 3 MPa. As a result of this, no cracking in the slab was observed.

CHAPTER 5

CONCLUSION

In this study, two different mixes were fabricated, and their free shrinkage was tested according to ASTM C157, and restrained shrinkage performance in both ring test and a large-scale slab were assessed. In-situ strain measurement using vibrating wire strain gages was conducted to further evaluate the shrinkage behavior of concrete affected by various factors, including early age drying effect and restraining conditions. The following conclusions can be drawn from the study:

1) The restrained ring test reported the cracking of NC mix at approximately 3 days whereas for CPC mix it was seen to be 4 days. The delay of cracking was observed due to reduced cement content and reduced w/c ratio in CPC mix as compared to NC mix. Theoretically, the ring cracks when the residual stress in concrete reaches the tensile strength but, experimental evidence typically shows that cracking takes place at lower values.
2) The free shrinkage test results along with the regression coefficients shows that the degree of restraint provided by the ring for NC mix (70%) was higher than the CPC mix (60%) as the degree of restraint varies with time due to variation in elastic modulus. The degree of restraint varies by approximately 8-10% due to the differences in the elastic modulus. In addition, the comparison of w/c ratio of the two mixtures shows that the degree of restraint is higher when the w/c ratio is high.
3) The shrinkage strains obtained from the vibrating wire strain gages in slab shows that when the slab is restrained completely, the maximum movement of the slab is near the center. Similarly, unrestrained slab recorded maximum shrinkage at the

center of the slab. Whereas the comparison of unrestrained to restrained slab shows higher internal movements. Along the edge of the slab, the shrinkage strains increase towards the center of the slab and then decreases towards the other end of the slab.

4) The concrete cracks as the tensile stress within concrete reaches the tensile strength of the concrete. Here, the tensile stress developed in the slabs up to the age of 11 days was found out to be 1.65 MPa. However, the tensile strength obtained from ASTM C496 at the same age was about 3.2 MPa. As a result of this, no cracking was observed on the slab.

REFERENCES

[1] Aly, T., & Sanjayan, J. G. (2009). Mechanism of early age shrinkage of concretes. *Materials and Structures*, *42*(4), 461–468. https://doi.org/10.1617/s11527-008-9394-6

[2] Azenha, M., Faria, R., & Ferreira, D. (2009). Identification of early-age concrete temperatures and strains: Monitoring and numerical simulation. *Cement and Concrete Composites*, *31*(6), 369–378. https://doi.org/10.1016/j.cemconcomp.2009.03.004

[3] Bakhshi, M. (n.d.). *Characterization and Modeling of Moisture Flow through hydrating Cement-Based Materials under Early-Age Drying and Shrinkage Conditions* [Ph.D., Arizona State University]. Retrieved March 30, 2023, from https://www.proquest.com/docview/885869884/abstract/8FAA44321D24208PQ/1

[4] Bazant, Z. P. (1986). 4th RILEM International Symposium on Creep and Shrinkage of Concrete Mathematical Modeling. *Materials and Structures*, *19*(6), 459–459. https://doi.org/10.1007/BF02472152

[5] Beglarigale, A., Eyice, D., Tutkun, B., & Yazıcı, H. (2021). Evaluation of enhanced autogenous self-healing ability of UHPC mixtures. *Construction and Building Materials*, *280*, 122524. https://doi.org/10.1016/j.conbuildmat.2021.122524

[6] Bentur, A., N. S. Berke, M. P. D., & Durning, T. A. (2001). Crack Mitigation Effects of Shrinkage Reducing Admixtures. *Special Publication*, *204*, 155–170. https://doi.org/10.14359/10818

[7] Carlson, R. W. (1938). DRYING SHRINKAGE OF CONCRETE AS AFFECTED BY MANY FACTORS. *American Soc Testing & Materials Proc*. https://trid.trb.org/view/95702

[8] Carlson, R. W., & Reading, T. J. (1988). Model Study of Shrinkage Cracking in Concrete Building Walls. *Structural Journal*, *85*(4), 395–404. https://doi.org/10.14359/2666

[9] *Characterizing Effective Built-In Curling from Concrete Pavement Field Measurements | Journal of Transportation Engineering | Vol 131, No 4*. (n.d.). Retrieved April 7, 2023, from https://ascelibrary.org/doi/full/10.1061/%28ASCE%290733-947X%282005%29131%3A4%28320%29?casa_token=rTFaORod2soAAAAA%3AVky8E8cs0X5phl_aHl5vQKir0sFJmLFKb1cXSgGSXDBUjMhV9i2Idx6BYnDClTZX2ezXGqFLAYo

[10] *Drying Shrinkage, Curling, and Joint Opening of Slabs-on-Ground—ProQuest*. (n.d.). Retrieved March 30, 2023, from https://www.proquest.com/openview/350135c71bf15dbfa13f2d0620ad0665/1?casa_token=9cIIjd37KPQAAAAA:AqPHArPvkh48Ixay-luE3eZBIHYDEccsqOzQdyt_kQHewbez_HbNzkyT1p_HBuziEinWDmfowA&cbl=37076&pq-origsite=gscholar&parentSessionId=LRU32cWKz5%2BDlOtmP65XaOAR0Ft%2BPcWIsInbQBY1qU0%3D

[11] *Early Age Stresses and Debonding in Bonded Concrete Overlays—David A. Lange, Hak-Chul Shin, 2001*. (n.d.). Retrieved April 7, 2023, from https://journals.sagepub.com/doi/10.3141/1778-21

[12] Hlaing, T. P. (n.d.). *CONCRETE Microstructure, Properties and Materials*. Retrieved March 30, 2023, from https://www.academia.edu/39955059/CONCRETE_Microstructure_Properties_and_Materials

[13] Holt, E. E. (n.d.). *Early age autogenous shrinkage of concrete* [Ph.D., University of Washington]. Retrieved March 30, 2023, from https://www.proquest.com/docview/250789878/abstract/CA25B42F49D44915PQ/1

[14] Hossain, A. B., & Weiss, J. (2004). Assessing residual stress development and stress relaxation in restrained concrete ring specimens. *Cement and Concrete Composites*, *26*(5), 531–540. https://doi.org/10.1016/S0958-9465(03)00069-6

[15] Hossain, A. B., & Weiss, J. (2006). The role of specimen geometry and boundary conditions on stress development and cracking in the restrained ring test. *Cement and Concrete Research*, *36*(1), 189–199. https://doi.org/10.1016/j.cemconres.2004.06.043

[16] Justnes, H., Van Gemert, A., Verboven, F., & Sellevold, E. J. (1996). Total and external chemical shrinkage of low w/c ratio cement pastes. *Advances in Cement Research*, *8*(31), 121–126. https://doi.org/10.1680/adcr.1996.8.31.121

[17] Kraai, P. P. (1985). *A proposed test to determine the cracking potential due to drying shrinkage of concrete. Concrete construction, 30(9), 775-778.*

[18] Liu, Y., & Wei, Y. (2021). Internal curing efficiency and key properties of UHPC influenced by dry or prewetted calcined bauxite aggregate with different particle size. *Construction and Building Materials*, *312*, 125406. https://doi.org/10.1016/j.conbuildmat.2021.125406

[19] Liu, Y., Wei, Y., Ma, L., & Wang, L. (2022). Restrained shrinkage behavior of internally-cured UHPC using calcined bauxite aggregate in the ring test and UHPC-concrete composite slab. *Cement and Concrete Composites*, *134*, 104805. https://doi.org/10.1016/j.cemconcomp.2022.104805

[20] Mailvaganam, N., Springfield, J., Repette, W., & Taylor, D. (n.d.). *Curling of Concrete Slabs on Grade*.

[21] Mehta, P. Kumar and J.M. Monteiro,. (n.d.). *Concrete: Structure, Properties and Materials. 2nd Edition, Prentice Hall, Inc., 1993, 548 pp.*

[22] Miltenberger, M. A., & Attiogbe, E. K. (2002). Shrinkage-Based Analysis for Control-Joint Spacing in Slabs-on-Ground. *Structural Journal*, *99*(3), 352–359. https://doi.org/10.14359/11919

[23] Moon, J. H., & Weiss, J. (2006). Estimating residual stress in the restrained ring test under circumferential drying. *Cement and Concrete Composites*, *28*(5), 486–496. https://doi.org/10.1016/j.cemconcomp.2005.10.008

[24] Nagataki, S. (1970). Shrinkage and Shrinkage Restraints in Concrete Pavements. *Journal of the Structural Division*, *96*(7), 1333–1358. https://doi.org/10.1061/JSDEAG.0002619

[25] Nam, J.-H., Kim, S.-M., & Won, M. C. (1947). Measurement and Analysis of Early-Age Concrete Strains and Stresses. *Transportation Research Record*.

[26] Opsahl, O. A., & Kvam, S. F. (1982). *Betong med FE-stat-fiber (Concrete with FE-Steel Fibers). Report No. STF 65A82036, SINTEF Div. FCB, Tromdheim, Norway.*

[27] Padron, I., & Zollo, R. F. (1990). Effect of Synthetic Fibers on Volume Stability and Cracking of Portland Cement Concrete and Mortar. *Materials Journal*, *87*(4), 327–332. https://doi.org/10.14359/2027

[28] *(PDF) Design and Control of Concrete Mixtures*. (n.d.). Retrieved March 30, 2023, from https://www.researchgate.net/publication/284663491_Design_and_Control_of_Concrete_Mixtures

[29] Pease, B., Shah, H., ++ A., & Weiss, W. (2023). *Restrained shrinkage behavior of mixtures containing shrinkage reducing admixtures and fibers*.

[30] Pease, B., Shah, H., & Weiss, W. (2005). Shrinkage Behavior and Residual Stress Development in Mortar Containing Shrinkage Reducing Admixtures (SRA's). *ACI Spec. Publ. Concr. Admixtures*, *227*.

[31] RILEM. (n.d.-a). *RILEM - Publications*. Retrieved April 7, 2023, from https://www.rilem.net/publication/publication/28?id_papier=1972

[32] RILEM. (n.d.-b). *RILEM - Publications*. Retrieved April 7, 2023, from https://www.rilem.net/publication/publication/53?id_papier=4558

[33] Shaeles, C. A., & Hover, K. C. (1988). Influence of mix proportions and Construction Operations on Plastic Shrinkage Cracking in Thin Slabs. *Materials Journal*, *85*(6), 495–504. https://doi.org/10.14359/2242

[34] Shah, S. P., Weiss, W. J., & Yang, W. (1998). Shrinkage Cracking—Can It Be Prevented? *Concrete International*, *20*(4), 51–55.

[35] Sidney and young. (n.d.). *Concrete. Prentice-Hall, Inc., 1981, 671 pp*.

[36] *Standard Test Method for Compressive Strength of Cylindrical Concrete Specimens*. (n.d.). Retrieved April 7, 2023, from https://www.astm.org/c0039_c0039m-21.html

[37] *Standard Test Method for Determining Age at Cracking and Induced Tensile Stress Characteristics of Mortar and Concrete under Restrained Shrinkage*. (n.d.). Retrieved April 7, 2023, from https://www.astm.org/standards/c1581

[38] *Standard Test Method for Length Change Of Hardened Cement Mortar And Concrete*. (n.d.). Retrieved April 7, 2023, from https://www.astm.org/c0157-75.html

[39] *Standard Test Method for Splitting Tensile Strength of Cylindrical Concrete Specimens*. (n.d.). Retrieved April 7, 2023, from https://www.astm.org/c0496-96.html

[40] *Standard Test Method for Static Modulus of Elasticity and Poisson's Ratio of Concrete in Compression*. (n.d.). Retrieved April 7, 2023, from https://www.astm.org/c0469_c0469m-22.html

[41] Tazawa, E. (1999). *Autogenous Shrinkage of Concrete*. Japan Concrete Institute.

[42] Weiss, W. J., Yang, W., & Shah, S. P. (2000). Influence of Specimen Size/Geometry on Shrinkage Cracking of Rings. *Journal of Engineering Mechanics*, *126*(1), 93–101. https://doi.org/10.1061/(ASCE)0733-9399(2000)126:1(93)

[43] Wongtanakitcharoen, T., & Naaman, A. E. (2007). Unrestrained early age shrinkage of concrete with polypropylene, PVA, and carbon fibers. *Materials and Structures*, *40*(3), 289–300. https://doi.org/10.1617/s11527-006-9106-z

[44] Yoo, D.-Y., Park, J.-J., Kim, S.-W., & Yoon, Y.-S. (2014). Influence of ring size on the restrained shrinkage behavior of ultra high performance fiber reinforced concrete. *Materials and Structures*, *47*(7), 1161–1174. https://doi.org/10.1617/s11527-013-0119-0